Modification of GATA-2 Transcriptional Activity in Endothelial Cells by the SUMO E3 Ligase PIASy

Tae-Hwa Chun, Hiroshi Itoh, Lalitha Subramanian, Jorge A. Iñiguez-Lluhí, Kazuwa Nakao

Abstract—GATA sequences are required for the optimal expression of endothelial cell–specific genes, including endothelin-1 (ET-1). We have identified PIASy in a search for new GATA-2 interacting proteins that can regulate GATA-2–mediated endothelial gene expression. Notably, among the cell populations comprising vascular walls, PIASy mRNA is selectively expressed in endothelial cells, and its expression can be regulated by angiogenic growth factors. We show that GATA-2 is covalently modified by small ubiquitin-like modifier (SUMO)-1 and -2 and that PIASy, through its E3 SUMO ligase activity, preferentially enhances the conjugation of SUMO-2 to GATA-2. Through a functional analysis, we demonstrate that PIASy potently suppresses the activity of the GATA-2–dependent human ET-1 promoter in endothelial cells. The suppressive effect of PIASy requires the GATA-binding site in the ET-1 promoter and depends on its interaction with GATA-2, which requires both N-terminal (amino acids 1-183) and C-terminal (amino acids 414-510) sequences in PIASy. We conclude that PIASy enhances the conjugation of SUMO-2 to GATA-2 and that the interaction of PIASy with GATA-2 can modulate GATA-mediated ET-1 transcription activity in endothelial cells through a RING-like domain-independent mechanism. (*Circ Res.* 2003;92:1201-1208.)

Key Words: GATA-2 ■ endothelin-1 ■ SUMO ligase ■ PIAS family

GATA-2 is a member of the GATA family (GATA-1 to -6) of transcription factors and plays a critical role in hematopoietic and cardiovascular development by regulating the transcription of key cell-type specific target genes. GATA-2 is expressed abundantly in primitive hematopoietic cells, and its level gradually declines during their maturation into different blood cell types.[1] Moreover, GATA-2 is expressed in adult endothelial cells, where it plays key roles in the transcriptional regulation of endothelial-specific genes containing GATA-binding sites in their promoter regions.[2–5]

Endothelin-1 (ET-1) is a potent vasoconstrictor that is expressed exclusively in endothelial cells.[6] A GATA-binding site located in the promoter of the human ET-1 gene is necessary for the optimal expression of ET-1 in endothelial cells.[7,8] Several studies have also demonstrated the significance of GATA-binding sites for the optimal expression of other endothelial-specific genes, such as endothelial nitric oxide synthase,[2] von Willebrand factor,[3] KDR,[4] and platelet-endothelial cell adhesion molecule-1.[5]

It has been postulated that coactivators or corepressors of GATA-2 could influence GATA-2–regulated expression of endothelial-specific genes and contribute to their complex regulation.[3,5,8–10] In a search for new molecules that can regulate GATA-2 function in endothelial cells, we have identified PIASy as a protein that interacts with GATA-2. PIASy was originally cloned as a member of the PIAS family of regulators of STAT function.[11] Recent reports have highlighted the ability of PIAS family members to act as small ubiquitin-like modifier (SUMO) ligases.[12–14] We found that GATA-2 is modified by SUMO proteins and that PIASy enhances the extent of SUMOylation. Moreover, by examining the effect of PIASy on the promoter activity of the human ET-1 gene, we found that PIASy strongly represses ET-1 promoter activity through its interaction with GATA-2.

Materials and Methods

Plasmids

The human GATA-2 cDNA (1.7 kb) was obtained by reverse transcriptase–polymerase chain reaction (RT-PCR) from HEL cells. Yeast expression vectors are derivatives of the pBTM116 (Paul Bartel and Stanley Fields). N-terminal and C-terminal fragments of hGATA2 encoding aa 1-475 and 275-475 were subcloned into pBTM116 (pLexA-GATA2 and pLexA-GATA2ΔN). The expression vector for LexA-fused Val14 RhoA (pBTM-Val14-RhoA) was obtained from Naoki Watanabe (Kyoto University).[15] The GATA-2 cDNA was subcloned into pcDNA3.1-V5-His (Invitrogen). The pACT2-PIASy vector corresponds to one of the full-length isolates obtained through our yeast two-hybrid screening. The FLAG-tagged PIASy expression vector, pFLAG-PIASy, was constructed by inserting a *SalI/BglII* fragment of pACT2-PIASy into pFLAG-CMV-2 (Sigma). Expression vectors for the deletion mutants of PIASy, pFLAG-PIASyΔN (deletion of nt 0-472), pFLAG-PIASyΔM (nt 549-1242), and pFLAG-PIASyΔC (nt 669-1533) were created by restriction enzyme digestion and religation. Three copies of the SV40 nuclear localization signal (DKKKRKV) were inserted between the FLAG tag and PIASyΔC to create pFLAG-NLS-PIASyΔC. Inserting the SalI/BglII fragment of pACT2-PIASy into

Original received December 9, 2002; revision received April 7, 2003; accepted April 23, 2003.

From the Department of Medicine and Clinical Science (T.C., H.I., K.N.), Kyoto University Graduate School of Medicine, Kyoto, Japan, and Departments of Pharmacology (L.S., J.I.) and Internal Medicine (T.C., S.W.), University of Michigan Medical Center, Ann Arbor, Mich.

Correspondence to Tae-Hwa Chun, 5240 MSRBIII, 1150 W Medical Center Dr, Ann Arbor, MI 48109. E-mail taehwa@umich.edu

Circulation Research is available at http://www.circresaha.org

DOI: 10.1161/01.RES.0000076893.70898.36

pGEX4T3 (Pharmacia) yielded pGST-PIASy. pcDNA3-HA-SUMO-1 and pcDNA3-HA-SUMO-2/SMT3B were gifts of Kim Orth (UT Southwestern University, Dallas, Tex).[16]

The human ET-1 promoter (bp −204 to+180) was PCR amplified from human genomic DNA using forward (5′-CTGCCCCCGAATTGTCAGAC-3′) and reverse (5′-CGGGTTCCTCAGATCTCAAA-3′) primers (WT ET-1 promoter). Mutagenesis of the GATA and AP-1 sites was achieved by PCR and changed the GATA and AP-1-binding sequences 5′-TTATCT-3′ and 5′-GTGACTAA-3′ to 5′-GTATAC-3′ (GATA-mut) and 5′-TTAATTAA-3′ (AP-mut) respectively. The promoter fragments were ligated into pGL2 basic (Promega) to yield (pGL-wild ET, pGL-GATA-mut ET, and pGL-AP-mut ET, respectively).

Yeast Two-Hybrid Screening

The yeast reporter strain L40 was transformed sequentially with pLexA-hGATA2ΔN and a human placenta matchmaker cDNA library (Clontech) that produces fusion proteins with the GAL 4 activating domain. Candidate clones were identified as histidine prototrophs and as positive for Lac-Z. To confirm the specificity of the association, candidate clones were cured of bait plasmid and mated with the yeast strain AMR70 harboring pLexA-GATA2, pLexA-GATA2ΔN, or pBTM-Val14-RhoA. Yeast strains were obtained from Stanley Hollenberg.

Immunoprecipitation, Western Blot, and Immunofluorescence

Transfection of COS 1 cells with empty pFLAG-CMV2 vector, pFLAG-PIASy, -PIASyΔM, -PIASyΔC, -PIASyΔN, or NLS-PIASyΔC together with pcDNA3.1-V5-His vector or pcDNA-GATA2-V5-His was performed with Lipofectamine (Gibco). Cell lysates were prepared 48 hours after transfection in lysis buffer (20 mmol/L Tris-Cl, pH 7.4, 150 mmol/L NaCl, 1 mmol/L EDTA, 1% Triton X-100) with protease inhibitor cocktail (Sigma). Expression of GATA2-V5 and FLAG-tagged proteins was analyzed by Western blotting using anti-V5-HRP antibody (Invitrogen) or anti-FLAG Bio-M2 antibody (Sigma) followed by anti-biotin-HRP antibody, respectively. Immunoprecipitations were carried out for 1 to 2 hours at 4°C by adding 3 μg of anti-FLAG M2 antibody to cell lysates (500 μg) followed by an overnight incubation at 4°C with protein G-Sepharose (Amersham). Samples were washed four times with lysis buffer and subjected to SDS/PAGE on 7.5% gels, and V5-tagged proteins were visualized as described above.

Transfected COS 1 cells were seeded onto glass slides 24 hour after transfection. After an additional 24 hours, slides were fixed in 4% paraformaldehyde in TBS for 10 minutes and permeabilized with 0.5% Triton X-100 for 5 minutes. The slides were incubated overnight with FLAG M2 monoclonal antibody, and secondary detection was performed with Alexa Fluor 594 anti-mouse IgG (Molecular Probe). Nuclear structure and F-actin were visualized with Hoechst 33342 and Alexa Fluor 488-phalloidin (Molecular Probes), respectively.

SUMOylation Assay

HEK 293T cells were transfected with pcDNA-GATA2-V5-His and either pcDNA-HA-SUMO-1 or pcDNA-HA-SUMO-2 in the presence or absence of pFLAG-PIASy using Lipofectamine Plus. Cells were harvested 36 hours after transfection in 0.7 mL of urea lysis buffer (8 mol/L urea, 0.5 mol/L NaCl, 45 mmol/L Na_2HPO_4, 5 mmol/L NaH_2PO_4, 10 mmol/L imidazole, pH 8.0) and sonicated. Lysates were incubated with 0.1 mL of Ni-NTA agarose (Qiagen) for 1 hour at room temperature in a rotator. After three washes with buffer 1 (8 mol/L urea, 0.4 mol/L NaCl, 17.6 mmol/L Na_2HPO_4, 32.4 mmol/L NaH_2PO_4, 10 mmol/L imidazole, pH 6.75) and three washes with buffer 2 (buffer 1 with 150 mmol/L NaCl and no urea), samples were processed for immunoblotting using anti-V5 (Invitrogen) or anti-HA (Covance) antibodies followed by goat anti-mouse HRP conjugate.

Tissue Culture and Northern Blot Analysis

A C57BL6 mouse was killed according to Kyoto University's Animal Rights Guidelines, and tissue RNA was isolated using Trizol reagents (GiboBRL). Human tissue blots were obtained from Clontech. Mouse vascular endothelial cells isolated from skin dermis[17] were obtained from Hedwig Murphy (University of Michigan, Ann Arbor, Mich) and characterized by von Willebrand factor, platelet-endothelial cell adhesion molecule-1, and VE-cadherin staining. Isolated mouse vascular smooth muscle cells[18] homogeneously expressing smooth muscle 22α, calponin, and smooth muscle-actin were obtained from S. Filippov (University of Michigan). Skin fibroblasts were obtained from F. Sabeh (University of Michigan). Bovine carotid endothelial cells (BAECs) were isolated as previously described.[19] Cells were maintained in DMEM with 10% FCS. BAECs were serum-starved for 24 hours before stimulation with 50 ng/mL human vascular endothelial growth factor (VEGF), 10 ng/mL basic fibroblast growth factor (bFGF), or 10% serum. Total RNA was prepared as above, and Northern blots were probed with a radiolabeled *Bgl*II fragment of pACT2-PIASy.

ET-1 Promoter Luciferase Reporter Assay in BAECs and Hela Cells

BAECs or Hela cells cultured in 12-well dishes were transfected with reporter plasmids, pGL-wild ET-1, -GATA-mut ET-1, or -AP-mut ET-1 together with the expression vectors, pFLAG-PIASy, or pcDNA-GATA2-V5. All experiments were controlled with the appropriate empty vectors. Luciferase activities were measured 48 hours after transfection according to the manufacturer's protocol (Promega). Parallel transfections using pRL-CMV vector (Promega) and assaying for Renilla luciferase indicated that transfection efficiency did not vary by >10%.

Electrophoretic Gel Mobility Shift Assay

Recombinant GST-PIASy was purified from XL-1 blue cells (Stratagene) transformed with pGST-PIASy. After 8 hours of induction with IPTG, the GST-fusion proteins were purified by glutathione-Sepharose chromatography according to the manufacturer's protocol (Amersham).

Crude mini-nuclear extracts from BAECs were prepared as described previously.[20] GATA consensus (CACTTGATAACAGAAAGTGATAACTCT) or mutant oligonucleotides (CACTTCTTAACAGAAAGTCTTAACTCT) (50 ng, Santa Cruz) were end-labeled with γ-[^{32}P]-ATP and T4 kinase (Takara Shuzo). Nuclear extracts (6 μg) were mixed with 2 μL (2 ng) of end-labeled oligonucleotide probes, 1 μg of poly(dI-dC) (Amersham), and the indicated amounts of GST-PIASy in binding buffer (10 mmol/L HEPES, 50 mmol/L KCl, 5 mmol/L MgCl2, 1 mmol/L EDTA, 5% glycerol). After a 20-minute incubation on ice, samples were resolved by electrophoresis in 0.5×TBE 7.5% polyacrylamide gels. Complexes were visualized by autoradiography.

Results

PIASy Interacts With GATA-2

To search for candidate proteins that regulate GATA-2–mediated endothelial gene expression, we used the yeast two-hybrid method to identify GATA-2 interacting proteins. Screening of 3×10^6 colonies transformed with human placenta GAL4 activation domain fusion cDNA libraries yielded 45 candidates. Subsequent mating assays revealed that five clones exhibited a specific interaction with LexA-fused to full length GATA-2 (aa 1-475) or the C-terminal half of GATA-2 (GATA2ΔN, aa 275-475). These clones did not interact with the control LexA-Val14-RhoA fusion (Figure 1A). The entire nucleotide sequences of two clones were identical, and a BLASTN search of the GenBank database identified the insert as the full-length cDNA of human PIASy.[11]

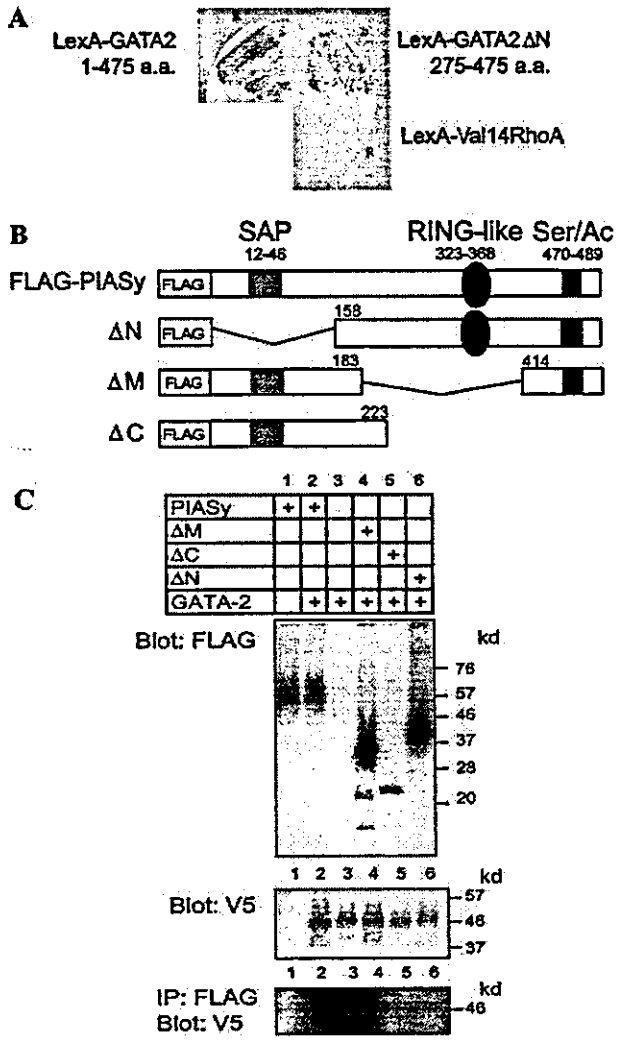

Figure 1. Interaction of PIASy with GATA-2. A, Yeast two-hybrid assay showing the interaction of PIASy with LexA-fused GATA-2 (aa 1-475) and GATA-2ΔN (aa 275-475). Val14RhoA is used as a negative control. B, Structure of FLAG-PIASy (aa 1-510) and its deletion mutants, PIASyΔN (aa 158-510), PIASyΔM (aa 1-183 and 414-510), and PIASyΔC (aa 1-223) are shown. PIASy contains a scaffold-associated region (SAR)-specific bipartite DNA-binding domain at aa 12-46, a RING finger–like domain (RING-like) at 323-368, and the serine-rich acidic domain (Ser/Ac) at 470-492. C, Interaction of FLAG-PIASy or its deletion mutants with GATA2-V5. COS 1 cells were transfected with pFLAG-PIASy (lanes 1 and 2), pFLAG-CMV–null vector (lane 3), pFLAG-PIASyΔM (lane 4), pFLAG-PIASyΔC (lane 5), or pFLAG-PIASyΔN (lane 6) with pcDNA-V5–null vector (lane 1) or pcDNA-GATA2-V5 (lanes 2 through 6). Cells were harvested 48 hours after transfection, and 20 μg of total cell lysates was blotted with anti-FLAG M2-Bio antibody (top) and anti-V5-HRP antibody (middle). Total cell lysates (500 μg) were immunoprecipitated with anti-FLAG-M2 antibody and blotted with anti-V5-HRP antibody (bottom).

PIASy is a member of the Protein Inhibitor of Activated Stat (PIAS) family of proteins, the founding members of which were initially described as negative regulators of STAT function. PIASy contains a scaffold-associated region (SAR)-specific bipartite DNA-binding domain at amino acids (aa) 12 to 46,[21] a RING finger–like domain at 323-368,[12,22] and a serine-rich acidic domain (Ser/Ac) at 470-492[11,13] (Figure 1B).

To confirm the interaction of PIASy with GATA-2 in mammalian cells, expression vectors for N-terminally FLAG-tagged PIASy (FLAG-PIASy) or three deletion mutants, ie, PIASy ΔM, ΔC, and ΔN (Figure 1B), were transfected into COS 1 cells together with the expression vector for GATA-2. GATA-2 was specifically coimmunoprecipitated with an anti-FLAG antibody in complex with the full-length FLAG-PIASy (Figure 1C, lane 2). The deletion of aa 183-413 encompassing the RING domain (FLAG-PIASyΔM) did not affect the interaction with GATA-2 (lane 4). In contrast, deletion of the entire C-terminal half of PIASy (Δ224-510, FLAG-PIASyΔC) or the first 157 aa (PIASyΔN) significantly reduced the interaction (lanes 5 and 6). This analysis suggests that the interaction between GATA-2 and PIASy involves the C-terminal region of GATA-2 and both amino (1-157) and C terminal (414-510) determinants in PIASy. Examination of the subcellular localization of PIASy by confocal microscopy showed that PIASy localizes to the nucleus and is enriched at the nuclear envelope. This was confirmed through costaining with the DNA dye Hoechst 33342 and visualization of the cell contour by staining for cortical actin (Figures 2A through 2E). Deletion of the N-terminal domain, which contributes to the interaction with GATA-2, did not affect the PIASy nuclear localization (Figure 2F). The PIASyΔM construct lacking the RING domain still localized to the nucleus, but the association with the nuclear envelope appeared weaker (Figure 2G). Deletion of the C-terminal half of PIASy (PIASy ΔC) shifted the localization of the protein to the cytoplasm, suggesting that this region harbors a nuclear localization signal (Figure 2H). To examine whether the reduced interaction of PIASy ΔC with GATA-2 (Figure 1C) is attributable to its cytoplasmic localization, we inserted three SV40-derived nuclear localization signals between the FLAG-tag and PIASyΔC (NLS-ΔC). This operation restored nuclear localization to PIASy ΔC (Figure 2I). The interaction of this construct with GATA2, however, remained marginal (Figure 2J).

Expression of PIASy in Endothelial Cells

PIASy mRNA was observed ubiquitously in several mouse tissues (Figure 3A) with testis showing substantially higher levels. A similar expression pattern was observed in human tissue blots (data not shown). Given our interest in the role of PIASy in the regulation of endothelial gene expression, we examined PIASy mRNA levels in individual cell types of the vascular wall. PIASy mRNA was readily detectable in isolated vascular endothelial cells, whereas expression was much weaker in smooth muscle cells and fibroblasts (Figure 3B). This pattern of expression is similar to that of GATA2 and indicates that in the vascular wall, PIASy may play a role in regulating endothelial-specific processes. To examine the possible regulation of PIASy mRNA expression, BAECs were stimulated with VEGF, bFGF, or FCS. All three stimuli augmented expression of PIASy mRNA significantly (Figure 3C). The existence of a regulatory mechanism to upregulate PIASy suggests that this protein may alter the function of activated endothelial cells.

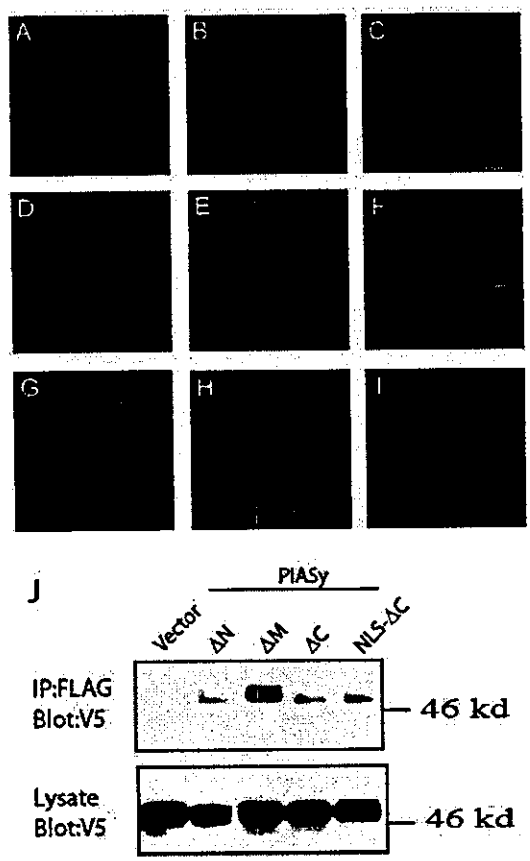

Figure 2. Subcellular localization of PIASy and its mutant COS 1 cells were transfected with pFLAG-PIASy, pFLAG-PIASyΔN, pFLAG-PIASyΔM, pFLAG-PIASyΔC, or pFLAG-NLS-PIASyΔC. Cells were processed for immunofluorescence 36 hours after transfection, as described in Materials and Methods. A, Anti-FLAG staining (red) in COS-1 cells transfected with full-length PIASy. B, Image from panel A merged with an image of Hoechst 33342 nuclear staining (blue). C, Confocal image of cells stained for PIASy (red) and F-actin (green). D through I, COS-1 cells transfected with control FLAG-CMV vector (D), full-length PIASy (E), PIASyΔN (F), PIASyΔM (G), PIASyΔC (H), and NLS-PIASyΔC (I) were stained for the FLAG-epitope (red) and F-actin (green). J, The interaction of FLAG-PIASy deletion mutants as well as a nucleus-localized form of PIASyΔC (NLSΔC) with GATA2 were examined as in panel C.

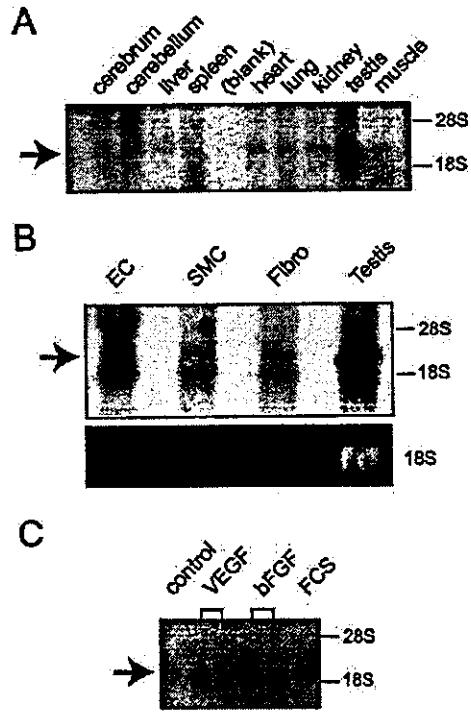

Figure 3. Selective and regulated expression of PIASy mRNA. A, Tissue distribution of PIASy mRNA was examined by Northern blot analysis using 20 μg total RNA from mouse tissues. Hybridized bands were indicated with an arrow. B, Expression of PIASy mRNA in different vascular wall cell types. Northern blot analysis was performed using 20 μg total RNA from mouse vascular endothelial cells (EC), smooth muscle cells (SMC), and fibroblasts (Fibro). RNA from mouse testis was used as positive control. C, Bovine endothelial cells were stimulated with VEGF 50 ng/mL, bFGF 10 ng/mL, or FCS 10% for 6 hours, and total RNA (20 μg) prepared from each sample was examined for PIASy mRNA expression. The effect of VEGF and bFGF was examined in duplicate.

PIASy Enhances SUMO Conjugation to GATA-2

Recent findings suggest that PIAS family members function as SUMO ligases.[13] Given that PIASy interacts with GATA-2, we examined if GATA-2 is SUMOylated and whether PIASy can promote the extent of its modification. HEK 293T cells were cotransfected with GATA-2-V5-His and HA-SUMO-1 or HA-SUMO-2 in the absence or presence of PIASy. GATA-2 was then purified under denaturing conditions via Ni-NTA chromatography. Western blot analysis demonstrated equal recovery of GATA-2 in all conditions (Figure 4A, left). In addition, minor slowly migrating bands could be detected, particularly from cells that were cotransfected with SUMO-2 and PIASy (Figure 4A, left). Probing the same samples for HA immunoreactivity demonstrated that the upper bands correspond to SUMO-conjugated GATA-2 (Figure 4A, right). Notably, the SUMO-2 conjugated form of GATA-2 was strongly enhanced by PIASy (Figure 4A, right). Probing of the crude extracts with the anti-HA antibody revealed that PIASy enhances the SUMO modification of multiple cellular proteins. As in the case of GATA-2, a stronger effect is observed for SUMO-2 (Figure 4B, right). Flag immunoblots clearly demonstrate the appropriate expression of PIASy (Figure 3B, left). These results show that GATA-2 is a target for SUMO modification and that PIASy enhances the SUMO conjugation of GATA-2, especially by SUMO-2.

Suppression of ET-1 Promoter Activity by PIASy in Endothelial Cells

We next examined whether PIASy affects GATA-2–mediated gene regulation in endothelial cells. We chose the ET-1 promoter because its activity has been well characterized and is a clear example of GATA-mediated endothelial gene regulation.[7,8,23] To assess the effect of PIASy on the ET-1 promoter, we constructed luciferase reporter constructs containing the proximal promoter region (bp −202 to +180) of the human ET-1 gene, which contains single GATA (TTATCT, bp −136 to −131) and AP-1 (TGACTAA, bp −108 to −102) binding sites. Transfection of GATA-2 upregulated the ET-1 promoter activity in BAECs dose-

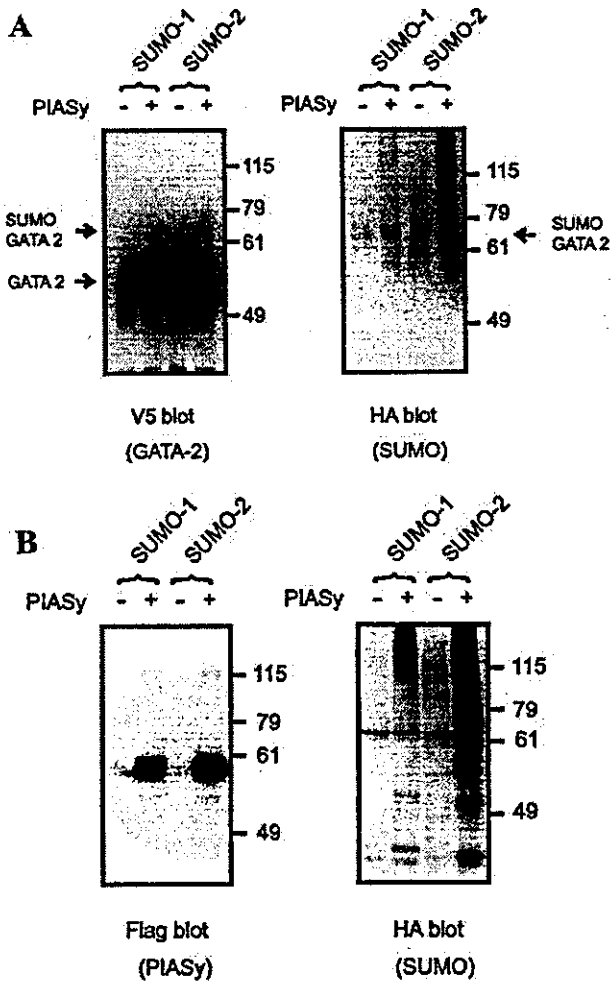

Figure 4. SUMOylation of GATA-2 by PIASy. A, HEK 293T cells were transfected with GATA-2-V5-His and either HA-SUMO-1 or HA-SUMO-2 in the absence or presence of PIASy. GATA-2 was purified as described in Materials and Methods. Samples were resolved by SDS PAGE and blotted with anti-V5 antibody (left) to detect GATA-2 and with an anti-HA antibody (right) to detect SUMO-1 or SUMO-2. The positions of unmodified GATA-2 (lower arrow) as well as a slowly migrating SUMOylated form of GATA-2 (upper arrow) are indicated. B, Total cell lysates were resolved and blotted with an anti-FLAG antibody (left) to detect the expression of PIASy and an anti-HA antibody (right) to detect total SUMO-1 or SUMO-2-modified proteins.

dependently (Figure 5A). When PIASy was cotransfected, the effect of GATA-2 on ET-1 promoter activity was no longer observed (Figure 5A). Cotransfection of increasing amounts of PIASy showed a dose-dependent suppression of ET-1 promoter activity in endothelial cells (Figure 5B). To examine the role of specific PIASy regions on the GATA-dependent transcription regulation of the ET-1 promoter, we tested the individual PIASy deletion mutants in endothelial cells. The RING-like domain deleted PIASy (PIASyΔM), which still interacted with GATA-2, showed the suppressive effect on ET-1 promoter activity (Figure 5C). Deletion of the entire C-terminal domain (PIASyΔC) abolished the inhibitory effect on ET-1 promoter activity. As in the case of GATA-2 interaction, this lack of suppression was not attributable to the impaired nuclear localization, because shifting its localization to the nucleus by addition of three copies of the SV40 NLS (Figure 2I) did not restore inhibition of the ET-1 promoter (Figure 5C). The N-terminally deleted mutant (PIASyΔN), which appeared to interact only feebly with GATA-2, did not retain any suppressive effect on ET-1 promoter activity but rather enhanced the basal ET-1 promoter activity. The correlation between GATA-2 binding and inhibition of the ET-1 promoter suggests that the physical interaction between PIASy and GATA-2 involving both N-terminal and C-terminal regions is important in the control of ET-1 promoter activity. Furthermore, the RING-like domain is dispensable for the interaction and ET-1 promoter inhibition.

To examine the cell specificity of the PIASy-mediated suppression of the ET-1 promoter, we examined the effect of PIASy in Hela cells expressing GATA-2. The basal activity of the ET-1 promoter in Hela cells is less than one tenth the activity in endothelial cells. Contrary to endothelial cells, expression of PIASy in Hela cells did not show any inhibitory effect on the ET-1 promoter activity (Figure 5D). Similar results were obtained in COS 1 cells (data not shown). This suggests that PIASy-mediated suppression of ET-1 promoter activity is specific to endothelial cells.

GATA Binding Site–Dependent Suppression of ET-1 Promoter Activity by PIASy

To investigate the sites in the ET-1 promoter responsible for the repressive effect of PIASy, we mutated the GATA site (bp −136 to −131) or the AP-1 site (bp −136 to −131) in the ET-1 promoter. The basal luciferase activity of the GATA site–mutated and AP-1 site–mutated ET-1 promoters in BAECs was approximately one half and one fourth of that observed with the WT ET-1 promoter, respectively. Consistent with the results shown in Figure 4, PIASy inhibited the WT ET-1 promoter substantially (Figure 6, left). In contrast, the GATA site–mutated ET-1 promoter displayed lower activity and was resistant to the repressive effect of PIASy (Figure 6, center). Although mutation of the AP-1 binding site in the ET-1 promoter reduced overall activity, the ability of PIASy to repress was still observable in this context (Figure 6, right).

PIASy Does Not Alter the GATA Sequence Binding Activity of Endothelial Cells

PIAS1 and PIAS3 have been reported to inhibit the DNA-binding activity of STAT1 and STAT3.[24] We therefore examined whether a similar mechanism contributes to the suppressive effects of PIASy on GATA-2 function. Nuclear extracts from BAECs were incubated with increasing amounts of purified GST-PIASy or GST alone, and the mixtures were analyzed by EMSA using a radiolabeled GATA-2 consensus double-stranded oligonucleotide as probe. BAEC nuclear extracts showed binding activity with the radiolabeled wild-type GATA probe but not with a GATA-site mutant probe (Figure 7, lanes 1 and 2). The specificity of the binding was confirmed by competition with a 40-fold excess of unlabeled GATA probe (lane 3). In our experiments, addition of increasing amounts of GST or GST-

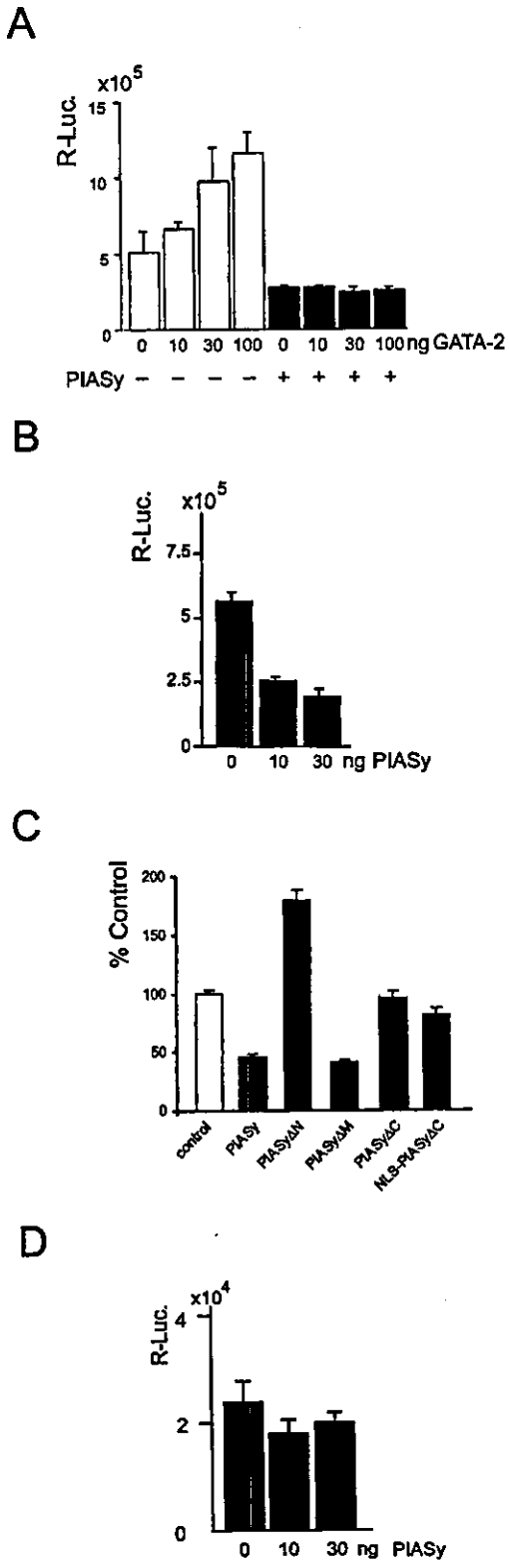

Figure 5. Suppression of the ET-1 promoter activity by PIASy in endothelial cells. A, BAECs were transfected with the WT ET-1 promoter luciferase reporter, and increasing amounts of pcDNA-GATA2-V5 in the absence (open columns) or presence (filled columns) of 30 ng pFLAG-PIASy. Luciferase activity was measured 48 hours after transfection. B, BAECs were transfected as in panel A, with the indicated amounts of pFLAG-PIASy and 100 ng pcDNA-GATA2-V5. C, WT ET-1 promoter activities were measured for the BAECs transfected with 30 ng of either empty vector (open bar) or expression vectors for the indicated PIASy forms together with 100 ng of pcDNA-GATA2-V5. The relative ET-1 promoter activities are normalized to the vector alone value, which was set to 100%. D, HeLa cells were transfected with the same plasmids as in B. Error bars represent 1 SD from the mean.

PIASy to the BAEC nuclear extracts did not affect the GATA DNA-binding activity significantly (lanes 4 through 9).

Discussion

In this study, we have identified an interaction between GATA-2 and PIASy and delineated the general requirements for this interaction. We have shown that PIASy expression is regulated in endothelial cells and have confirmed its SUMO E3 ligase activity. We also demonstrated that GATA-2 is covalently modified by SUMO and that PIASy enhances this modification. Notably, PIASy potently suppressed GATA-2–dependent ET-1 promoter activity in endothelial cells without altering GATA-2 DNA binding. The inhibitory effect required the same regions in PIASy implicated in its interaction with GATA-2.

Based on our two-hybrid data, both a full-length and an N-terminally–deleted GATA-2 interact with PIASy. This suggests that GATA-2 regions crucial to the interaction lie in the C-terminal region of GATA-2 (275-475 aa), which contains two zinc-finger domains. Our PIASy deletion-mutant analysis revealed that the interaction of PIASy with GATA-2 does not require its RING domain. Rather, the interaction requires both N-terminal (1-188 aa) and C-terminal (414-510 aa) sequences. The N-terminal domain of PIASy contains a scaffold-associated region (SAR)-specific bipartite DNA-binding domain, which is involved in binding to scaffold-associated regions of chromosomes.[21] SARs or otherwise called matrix attachment regions are anchorage sites within chromosome loops that possesses high affinity to nuclear matrix proteins,[25] including lamin.[26] Lamin is a major component of the nuclear lamina structure, and the DNA-binding activities of SP-1, ATF, CCAAT, C/EBP, OCT-1, and AP-1 have been reported to be enriched in these regions.[27] Consistent with its SAR binding properties, we detected an interaction between PIASy and lamin C by the yeast two-hybrid assay (data not shown). Notably, a colocalization of GATA-1 and lamin A in erythroleukemia cells has been already reported.[28] It is intriguing to consider that by interacting with both the nuclear lamina and GATA-2, PIASy could lead to the localization of GATA-2 in the proximity of other nuclear lamina-related transcription factors. We are presently examining this issue.

Our findings that among vascular wall cell types, PIASy is selectively expressed in endothelial cells, coupled with the observations that PIASy mRNA can be upregulated by angiogenic growth factors, indicate that PIASy and GATA-2 coexist in the endothelium and thus are likely to interact in their normal and pathophysiological context.

The PIAS family has been recently highlighted as E3 ligases for covalent conjugation of SUMO to target proteins.[29] Several transcription factors have been identified as

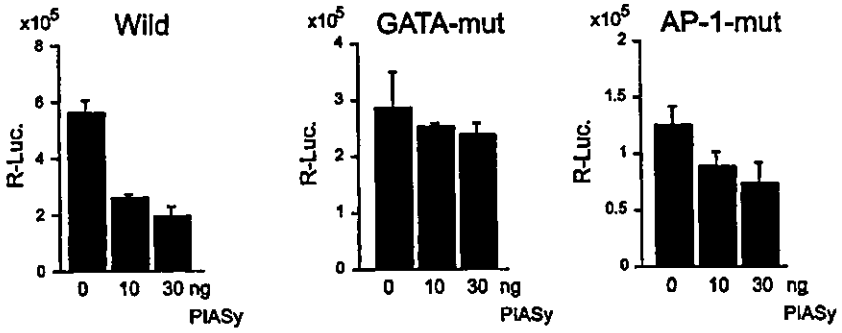

Figure 6. GATA binding site–dependent suppression of ET-1 promoter activity by PIASy. BAECs were transfected essentially as in Figure 5 with luciferase reporter plasmids driven by the WT ET-1 promoter (left) or ET-1 promoters with mutated GATA (center) or AP-1 (right) binding sites.

the target of PIAS-enhanced SUMOylation, including p53,[30] c-jun,[14] lymphoid enhancer factor 1,[13] androgen receptor,[31] and C/EBPα.[32] In this study, we could demonstrate that GATA-2 is SUMOylated and that PIASy can enhance the extent of this modification, especially in the case of the SUMO-2 isoform. Human GATA-2 contains two putative SUMOylation sites, MKME (aa 221-224) and MKKE (aa 388-391), that conform to the SUMOylation consensus sequence (ΨKXE, where Ψ represents a large hydrophobic amino acid).[33] These SUMOylation consensus sequences are conserved among other GATA family members from GATA-1 to GATA-6. Thus, SUMOylation of other GATA family members by PIAS proteins may occur in hematopoietic cells.

We have demonstrated that PIASy suppresses GATA-2–dependent ET-1 promoter activity in endothelial cells. The lack of inhibition observed in Hela and COS 1 cells indicates that the effect of PIASy on ET-1 promoter activity is selective to endothelial cells. This implies that additional endothelial-specific components beyond GATA-2 may be required for the inhibition of GATA-2 function by PIASy. Conversely, nonendothelial cells might contain factors that prevent PIASy from inhibiting GATA-2. Such factors could be additional proteins bridging or stabilizing the interaction between GATA-2 and PIASy or additional components of the SUMO conjugation pathway including SUMO proteases.[34]

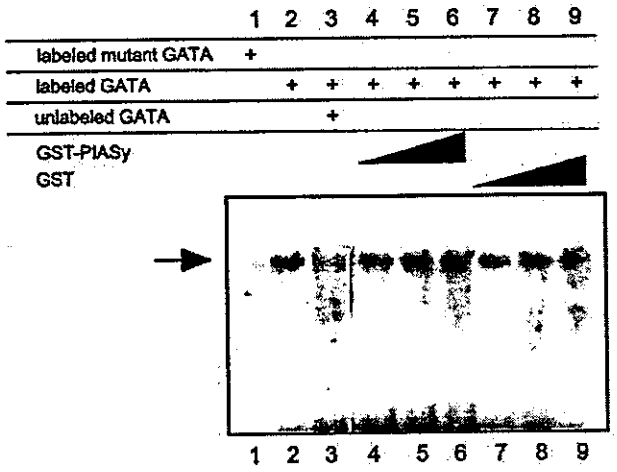

Figure 7. Effect of PIASy on DNA-binding activity of GATA. BAEC nuclear extracts were incubated with a radiolabeled GATA-mutant probe (lane 1) or a radiolabeled GATA-consensus probe (lanes 2 through 9). Reactions contained a 40-fold molar excess of unlabeled GATA consensus oligonucleotide probe (lane 3) or 0.05, 0.2, and 0.5 μg of purified GST-PIASy (lanes 4 through 6) or GST alone (lanes 7 through 9). Samples were resolved in a 7.5% polyacrylamide 0.5× TBE gel. The position of the GATA protein-DNA complex is indicated by the arrow.

Our deletion analysis results indicate that both N-terminal (aa 1-183) and C-terminal (aa 414-510) portions of PIASy are required for inhibition. These regions also correspond with those required for its interaction with GATA-2. Furthermore, the inhibitory effect of PIASy on the ET-1 promoter is mediated through the GATA binding sequence. Taken together, our results imply that the suppressive effect of PIASy on GATA-2 activity is attributable to the interaction between PIASy and GATA-2.

SUMO modification of transcription factors is often associated with reduced activity, and in some cases this seems to be attributable to reduced transcriptional synergy at promoters harboring multiple binding sites for the factor.[32] Here we showed that GATA-2 is SUMOylated, and PIASy enhances this modification. Notably, the ET-1 promoter used here harbors only a single GATA site, and in this context, the RING finger–like domain in PIASy, which is essential for its SUMO ligase activity, was dispensable for the repressive effect on the ET-1 promoter. Given that the inhibitory effect of SUMO modification of transcription factors may be restricted to promoters with multiple binding sites,[32] it is still possible that additional RING domain–dependent effects of PIASy on GATA-2 activity could be revealed at promoters harboring multiple GATA sites. Clearly, additional research is required to address the role of SUMO modification in the function of GATA-2 and its modification by PIASy.

In conclusion, we have identified PIASy as a GATA-2 interacting protein that enhances the SUMO conjugation of GATA-2. PIASy is expressed in endothelial cells and suppresses GATA-2–mediated ET-1 promoter activity in a cell-type–specific manner. Our findings reveal an additional level of complexity in the mechanisms by which GATA-2 regulates endothelial gene expression and suggest that manipulating the activity of transcriptional modifiers such as PIASy could be exploited to control endothelial function.

Acknowledgments

This study was supported by research grants from the Japanese Ministry of Education, Japanese Ministry of Health and Welfare, and Japanese Society for the Promotion of Science Research for the Future program (JSPS-RFTF 96100204, JSPS-RFTF98L00801). L.S. and J.I. acknowledge support from the American Heart Association (AHA 0225755Z and AHA 0130559Z) as well as from the

National Institute of Diabetes and Digestive and Kidney Diseases of the NIH (No. 5P60DK-20572). The authors thank Dr Stephen J. Weiss (University of Michigan) for his generous support and thoughtful suggestions. We also appreciate Mayumi Inoue (Kyoto University) for her helpful discussion and thank Keiko Kaya and Yasuko Nakagawa for their dedicated experimental assistance.

References

1. Tsai FY, Keller G, Kuo FC, Weiss M, Chen J, Rosenblatt M, Alt FW, Orkin SH. An early haematopoietic defect in mice lacking the transcription factor GATA-2. *Nature*. 1994;371:221–226.
2. Zhang R, Min W, Sessa WC. Functional analysis of the human endothelial nitric oxide synthase promoter: Sp1 and GATA factors are necessary for basal transcription in endothelial cells. *J Biol Chem*. 1995;270: 15320–15326.
3. Jahroudi N, Lynch DC. Endothelial-cell-specific regulation of von Willebrand factor gene expression. *Mol Cell Biol*. 1994;14:999–1008.
4. Patterson C, Perrella MA, Hsieh CM, Yoshizumi M, Lee ME, Haber E. Cloning and functional analysis of the promoter for KDR/flk-1, a receptor for vascular endothelial growth factor. *J Biol Chem*. 1995;270: 23111–23118.
5. Gumina RJ, Kirschbaum NE, Piotrowski K, Newman PJ. Characterization of the human platelet/endothelial cell adhesion molecule-1 promoter: identification of a GATA-2 binding element required for optimal transcriptional activity. *Blood*. 1997;89:1260–1269.
6. Yanagisawa M, Kurihara H, Kimura S, Tomobe Y, Kobayashi M, Mitsui Y, Yazaki Y, Goto K, Masaki T. A novel potent vasoconstrictor peptide produced by vascular endothelial cells. *Nature*. 1988;332:411–415.
7. Wilson DB, Dorfman DM, Orkin SH. A nonerythroid GATA-binding protein is required for function of the human preproendothelin-1 promoter in endothelial cells. *Mol Cell Biol*. 1990;10:4854–4862.
8. Kawana M, Lee ME, Quertermous EE, Quertermous T. Cooperative interaction of GATA-2 and AP1 regulates transcription of the endothelin-1 gene. *Mol Cell Biol*. 1995;15:4225–4231.
9. Tsang AP, Visvader JE, Turner CA, Fujiwara Y, Yu C, Weiss MJ, Crossley M, Orkin SH. FOG, a multitype zinc finger protein, acts as a cofactor for transcription factor GATA-1 in erythroid and megakaryocytic differentiation. *Cell*. 1997;90:109–119.
10. Svensson EC, Tufts RL, Polk CE, Leiden JM. Molecular cloning of FOG-2: a modulator of transcription factor GATA-4 in cardiomyocytes. *Proc Natl Acad Sci USA*. 1999;96:956–961.
11. Liu B, Liao J, Rao X, Kushner SA, Chung CD, Chang DD, Shuai K. Inhibition of Stat1-mediated gene activation by PIAS1. *Proc Natl Acad Sci USA*. 1998;95:10626–10631.
12. Kahyo T, Nishida T, Yasuda H. Involvement of PIAS1 in the sumoylation of tumor suppressor p53. *Mol Cell*. 2001;8:713–718.
13. Sachdev S, Bruhn L, Sieber H, Pichler A, Melchior F, Grosschedl R. PIASy, a nuclear matrix-associated SUMO E3 ligase, represses LEF1 activity by sequestration into nuclear bodies. *Genes Dev*. 2001;15: 3088–3103.
14. Schmidt D, Muller S. Members of the PIAS family act as SUMO ligases for c-Jun and p53 and repress p53 activity. *Proc Natl Acad Sci USA*. 2002;26:2872–2877.
15. Watanabe N, Madaule P, Reid T, Ishizaki T, Watanabe G, Kakizuka A, Saito Y, Nakao K, Jockusch BM, Narumiya S. p140mDia, a mammalian homolog of Drosophila diaphanous, is a target protein for Rho small GTPase and is a ligand for profilin. *EMBO J*. 1997;16:3044–3056.
16. Orth K, Xu Z, Mudgett MB, Bao ZQ, Palmer LE, Bliska JB, Mangel WF, Staskawicz B, Dixon JE. Disruption of signaling by Yersinia effector YopJ, a ubiquitin-like protein protease. *Science*. 2000;290:1594–1597.
17. Murphy HS, Bakopoulos N, Dame MK, Varani J, Ward PA. Heterogeneity of vascular endothelial cells: differences in susceptibility to neutrophil-mediated injury. *Microvasc Res*. 1998;56:203–211.
18. Ray JL, Leach R, Herbert JM, Benson M. Isolation of vascular smooth muscle cells from a single murine aorta. *Methods Cell Sci*. 2001;23: 185–188.
19. Suga S, Nakao K, Itoh H, Komatsu Y, Ogawa Y, Hama N, Imura H. Endothelial production of C-type natriuretic peptide and its marked augmentation by transforming growth factor-β: possible existence of "vascular natriuretic peptide system." *J Clin Invest*. 1992;90:1145–1149.
20. Schreiber E, Matthias P, Muller MM, Schaffner W. Rapid detection of octamer binding proteins with "mini-extracts," prepared from a small number of cells. *Nucleic Acids Res*. 1989;17:6419.
21. Gohring F, Schwab BL, Nicotera P, Leist M, Fackelmayer FO. The novel SAR-binding domain of scaffold attachment factor A (SAF-A) is a target in apoptotic nuclear breakdown. *EMBO J*. 1997;16:7361–7371.
22. Joazeiro CA, Weissman AM. RING finger proteins: mediators of ubiquitin ligase activity. *Cell*. 2000;102:549–552.
23. Lee ME, Bloch KD, Clifford JA, Quertermous T. Functional analysis of the endothelin-1 gene promoter: evidence for an endothelial cell-specific cis-acting sequence. *J Biol Chem*. 1990;265:10446–10450.
24. Chung CD, Liao J, Liu B, Rao X, Jay P, Berta P, Shuai K. Specific inhibition of Stat3 signal transduction by PIAS3. *Science*. 1997;278: 1803–1805.
25. Cockerill PN, Garrard WT. Chromosomal loop anchorage of the κ immunoglobulin gene occurs next to the enhancer in a region containing topoisomerase II sites. *Cell*. 1986;44:273–282.
26. Luderus ME, de Graaf A, Mattia E, den Blaauwen JL, Grande MA, de Jong L, van Driel R. Binding of matrix attachment regions to lamin B1. *Cell*. 1992;70:949–959.
27. van der Wijnen AJ, Bidwell JP, Fey EG, Penman S, Lian JB, Stein JL, Stein GS. Nuclear matrix association of multiple sequence-specific DNA binding activities related to SP-1, ATF, CCAAT, C/EBP, OCT-1, and AP-1. *Biochemistry*. 1993;32:8397–8402.
28. Neri LM, Raymond Y, Giordano A, Capitani S, Martelli AM. Lamin A is part of the internal nucleoskeleton of human erythroleukemia cells. *J Cell Physiol*. 1999;178:284–295.
29. Jackson PK. A new RING for SUMO: wrestling transcriptional responses into nuclear bodies with PIAS family E3 SUMO ligases. *Genes Dev*. 2001;15:3053–3058.
30. Megidish T, Xu JH, Xu CW. Activation of p53 by protein inhibitor of activated Stat1 (PIAS1). *J Biol Chem*. 2002;11:8255–8259.
31. Kotaja N, Karvonen U, Janne OA, Palvimo JJ. PIAS proteins modulate transcription factors by functioning as SUMO-1 ligases. *Mol Cell Biol*. 2002;22:5222–5234.
32. Subramanian L, Benson MD, Iniguez-Lluhi JA. A synergy control motif within the attenuator domain of CCAAT/enhancer-binding protein α inhibits transcriptional synergy through its PIASy-enhanced modification by SUMO-1 or SUMO-3. *J Biol Chem*. 2003;278:9134–9141.
33. Rodriguez MS, Dargemont C, Hay RT, Kaul S, Blackford JA Jr, Cho S, Simons SS Jr. SUMO-1 conjugation in vivo requires both a consensus modification motif and nuclear targeting. *J Biol Chem*. 2001;276: 12654–12659.
34. Best JL, Ganiatsas S, Agarwal S, Changou A, Salomoni P, Shirihai O, Meluh PB, Pandolfi PP, Zon LI. SUMO-1 protease-1 regulates gene transcription through PML. *Mol Cell*. 2002;10:843–855.

FEBS Letters 544 (2003) 86–92 FEBS 27287

Adrenomedullin provokes endothelial Akt activation and promotes vascular regeneration both in vitro and in vivo

Kazutoshi Miyashita, Hiroshi Itoh*, Naoki Sawada, Yasutomo Fukunaga, Masakatsu Sone, Kenichi Yamahara, Takami Yurugi-Kobayashi, Kwijun Park, Kazuwa Nakao

Department of Medicine and Clinical Science, Kyoto University Graduate School of Medicine, 54 Shogoin Kawahara-cho Sakyo-ku, Kyoto 606-8507, Japan

Received 18 February 2003; revised 14 April 2003; accepted 15 April 2003

First published online 14 May 2003

Edited by Beat Imhof

Abstract **We previously reported that adrenomedullin (AM), a vasodilating hormone secreted from blood vessels, promotes proliferation and migration of human umbilical vein endothelial cells (HUVECs). In this study, we examined the ability of AM to promote vascular regeneration. AM increased the phosphorylation of Akt in HUVECs and the effect was inhibited by the AM antagonists and the inhibitors for protein kinase A (PKA) or phosphatidylinositol 3-kinase (PI3K). AM promoted re-endothelialization in vitro of wounded monolayer of HUVECs and neo-vascularization in vivo in murine gel plugs. These effects were also inhibited by the AM antagonists and the inhibitors for PKA or PI3K. The findings suggest that AM plays significant roles in vascular regeneration, associated with PKA- and PI3K-dependent activation of Akt in endothelial cells, and possesses therapeutic potential for vascular injury and tissue ischemia.**

Key words: Adrenomedullin; cAMP; Akt; Angiogenesis; Re-endothelialization; Vascular regeneration

1. Introduction

Vascular regeneration is an essential event in recovery from endothelial injury or tissue ischemia. Thus, therapeutic strategies to promote re-endothelialization or neo-vascularization are now highlighted as promising treatment for atherosclerotic or ischemic diseases [1,2]. Many vasoactive substances secreted from endothelial cells (vascular hormones) have been reported to regulate not only vascular tone but also remodeling or regeneration. We revealed that C-type natriuretic peptide (CNP) is secreted from endothelial cells [3] and gene transfer of CNP promoted endothelial regeneration [4,5] and ischemia-induced angiogenesis [6] in vivo. We also reported that NPs directly promote endothelial regeneration in vitro [7]. In this way, NPs/cGMP/cGMP-dependent kinase (cGK) cascade is elucidated to be involved in the regulation of vascular regeneration.

Adrenomedullin (AM) is a potent vasorelaxant peptide that was originally isolated from human pheochromocytoma cells on the basis of its effect to elevate cAMP levels in rat platelets [8,9]. Recently, mice genetically engineered to overexpress or underexpress the AM gene were developed to determine the in vivo significance of AM [10–12]. Mice overexpressing the AM gene in their vasculature showed reduced blood pressure. On the other hand, mice lacking the AM gene did not survive the embryonic stage and showed abnormal vascular structure and subcutaneous hemorrhage. These observations suggest the significance of AM in vascular morphogenesis and regulation of vascular tone in vivo. AM has been shown to be present in atherosclerotic lesions and its secretion has been demonstrated to be augmented by inflammatory cytokines such as interleukin-1, TNF-α, and lipopolysaccharide [13]. Furthermore, hypoxia-responsive elements were identified in the AM gene and hypoxic conditions were reported to induce its expression and secretion from HUVECs [14]. These findings suggest the significance of AM for atherogenesis and angiogenesis.

Based on these findings, together with our recent report to show that AM enhanced proliferation and migration of cultured endothelial cells [15], we hypothesized that AM/cAMP/protein kinase A (PKA) cascade might have the potency to promote vascular regeneration. In this study, we tried to clarify whether AM has beneficial effects on vascular regeneration in the physiological in vitro model for endothelial regeneration and in vivo neo-vascularization in murine gel plugs.

2. Materials and methods

2.1. Materials and cell culture

All agents used were commercially available. Human AM, rat AM, proadrenomedullin N-terminal 20 peptide (PAMP), and the two AM antagonists, AM(22–52) and calcitonin gene-related peptide (8–37) (CGRP(8–37)) were purchased from the Peptide Institute (Osaka, Japan). The two PKA inhibitors, adenosine 3′,5′-cyclic monophosphorothioate Rp-isomer (Rp-cAMP) and myristoylated PKA inhibitor peptide sequence (14–22) cell-permeable (PKA Inh. Peptide), the two phosphatidylinositol 3-kinase (PI3K) inhibitors, LY294002 and wortmannin, and a cAMP analog, 8-Br-cAMP, were purchased from Calbiochem (San Diego, CA, USA). Vascular endothelial growth factor (VEGF) was purchased from Peprotech (London, UK).

HUVECs (Clonetics, Waltersville, MD, USA) were grown in the basic medium containing 2% fetal bovine serum (FBS) and growth supplements (EGM-2; Clonetics). Cell cultures between passages 4 and 6 were used for each experiment.

*Corresponding author. Fax: (81)-75-771 9452.
E-mail address: hiito@kuhp.kyoto-u.ac.jp (H. Itoh).

Abbreviations: AM, adrenomedullin; PKA, protein kinase A; PI3K, phosphatidylinositol 3-kinase; HUVEC, human umbilical vein endothelial cell; NP, natriuretic peptide; PKA Inh. Peptide, myristoylated protein kinase A inhibitor peptide sequence (14–22) cell-permeable; FBS, fetal bovine serum

0014-5793/03/$22.00
doi:10.1016/S0014-5793(03)00484-8

2.2. Western blot analysis of phosphorylated Akt

HUVECs were treated with or without AM (10^{-8} mol/l) and they were harvested 30 min after the treatments otherwise indicated. Western blotting was performed according to a standard protocol, as we described previously [16]. Akt activity was evaluated by the ratio of phosphorylated Akt to total Akt detected by phospho-Akt (Ser473) and Akt antibody (Cell Signaling, Beverly, MA, USA), respectively. To evaluate Akt activation in endothelial injury, artificial wounds were made by a blue-tip at intervals of 5 mm on an over-confluent monolayer of HUVECs. Densitometric assays were done and the results were presented as fold increase compared to the control.

2.3. Wound healing assay in vitro

To examine whether AM promotes endothelial regeneration in vitro, wound healing assay was carried out as we described previously [7]. In the report, we confirmed that this assay could evaluate overall activity of endothelial proliferation and migration. Briefly, HUVECs were grown to over-confluent in six-well plates and a wound of approximately 2 mm width was made by a cell scraper. Cells were allowed to repair the wound for 40 h in the medium containing 0.5% FBS with or without experimental agents. The wounded monolayer was photographed before and after the incubation period and the re-endothelialized area was evaluated.

2.4. Gel plug assay in vivo

To examine the ability of AM to induce neo-vascularization in vivo, we used murine MATRIGEL plug assay, as described previously [17]. Mice were handled with care according to accepted ethical guidelines. Nude mice were anesthetized with pentobarbiturate (80 mg/kg) and 400 μl per plug of growth factor-reduced phenol red-free MATRIGEL (Becton Dickinson, Bedford, MA, USA) was injected into the abdomen of 6–8 week old male KSN-nude mice (Japan SLC; Hamamatsu, Japan) subcutaneously. A mouse was injected two gels symmetrically in the abdomen, gels with and without experimental agents.

On day 0, 4, 7, 14, and 21, the margins of the subcutaneous plugs were marked and the mean blood flow and the size of the plugs were estimated by a laser Doppler perfusion image analyzer (Moor instruments, Devon, UK). Blood flow in the plug was calculated by the formula: (blood flow) = (mean blood flow) × (plug size). The ratio of the blood flow of the two plugs in the same mouse, an agent-containing plug to its control plug, was considered to be the index of the angiogenic activity of the agent.

The gel plugs were resected from mice on day 21 and stained with rat anti-mouse PECAM-1 (Pharmingen, San Diego, CA, USA) and the number of PECAM-1 positive cells in the plug was estimated as capillary density. 1-mm thick slices were also processed and stained with rat anti-mouse PECAM-1 and a fluorescent agent, Alexa Flour 488 conjugated goat anti-rat IgG (Molecular Probes, Eugene, OR, USA) for the observation with a confocal microscope (LSM5 PASCAL; Carl Zeiss, Oberkochen, Germany) that can reconstruct the 3D structure of the plug from the obtained consecutive images. In this way, small capillaries in the plug were visualized stereoscopically.

2.5. Statistics

All data are expressed as the mean ± S.E.M. Statistical analysis was performed with ANOVA (analysis of variance) or Student's *t*-test. Values of $P < 0.05$ were considered to be statistically significant.

3. Results

3.1. AM activated Akt in HUVECs in a PKA- and PI3K-dependent manner

Fig. 1A demonstrates a time course of the phosphorylation of Akt at amino acid residue 473 (serine) after the treatment with AM (10^{-8} mol/l) on HUVECs. Akt phosphorylation was augmented within 15 min and peaked at 30 min.

To examine Akt activation in endothelial damage, we made artificial wounds in a confluent monolayer of HUVECs as described in Section 2. The endothelial injury itself increased Akt phosphorylation and the addition of AM to the injured endothelium further augmented the increase (Fig. 1B).

AM-induced phosphorylation of Akt was inhibited by the two AM antagonists, AM(22–52) (10^{-5} mol/l) and CGRP-(8–37) (10^{-5} mol/l). The PKA inhibitors, Rp-cAMP (10^{-5} mol/l) and PKA Inh. Peptide (5×10^{-7} mol/l), and the inhibitors for PI3K, LY294002 (10^{-5} mol/l) and wortmannin (10^{-7} mol/l), also suppressed Akt phosphorylation significantly (Fig. 1C).

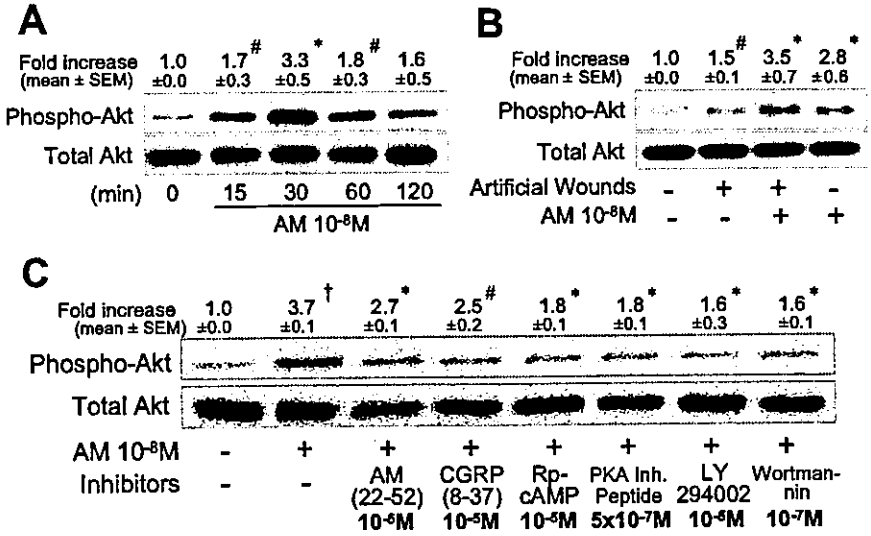

Fig. 1. Effect of AM on Akt activation in HUVECs. A: Time course of Akt phosphorylation in AM-treated HUVECs. Cells were treated with AM (10^{-8} mol/l) and harvested at the indicated times. B: Effect of artificial wounds and AM on Akt phosphorylation. Wounds were made at intervals of 5 mm on an over-confluent monolayer of HUVECs treated with or without AM. Cells were harvested 30 min after the treatments and phosphorylated Akt was detected. C: Effect of the AM antagonists and the inhibitors for PKA or PI3K on AM-induced Akt phosphorylation in HUVECs. Cells were pre-incubated with these inhibitors for 15 min before the administration of AM. They were harvested 30 min after the treatment and phosphorylated Akt was detected. Densitometric analyses were done and the ratio of phosphorylated Akt to total Akt is presented as fold increases compared to the control. #: $P < 0.05$; *: $P < 0.01$ versus the control (panels A and B) or the AM-treated group without inhibitors (panel C); †: $P < 0.01$ versus the control (panel C), $n = 3$.

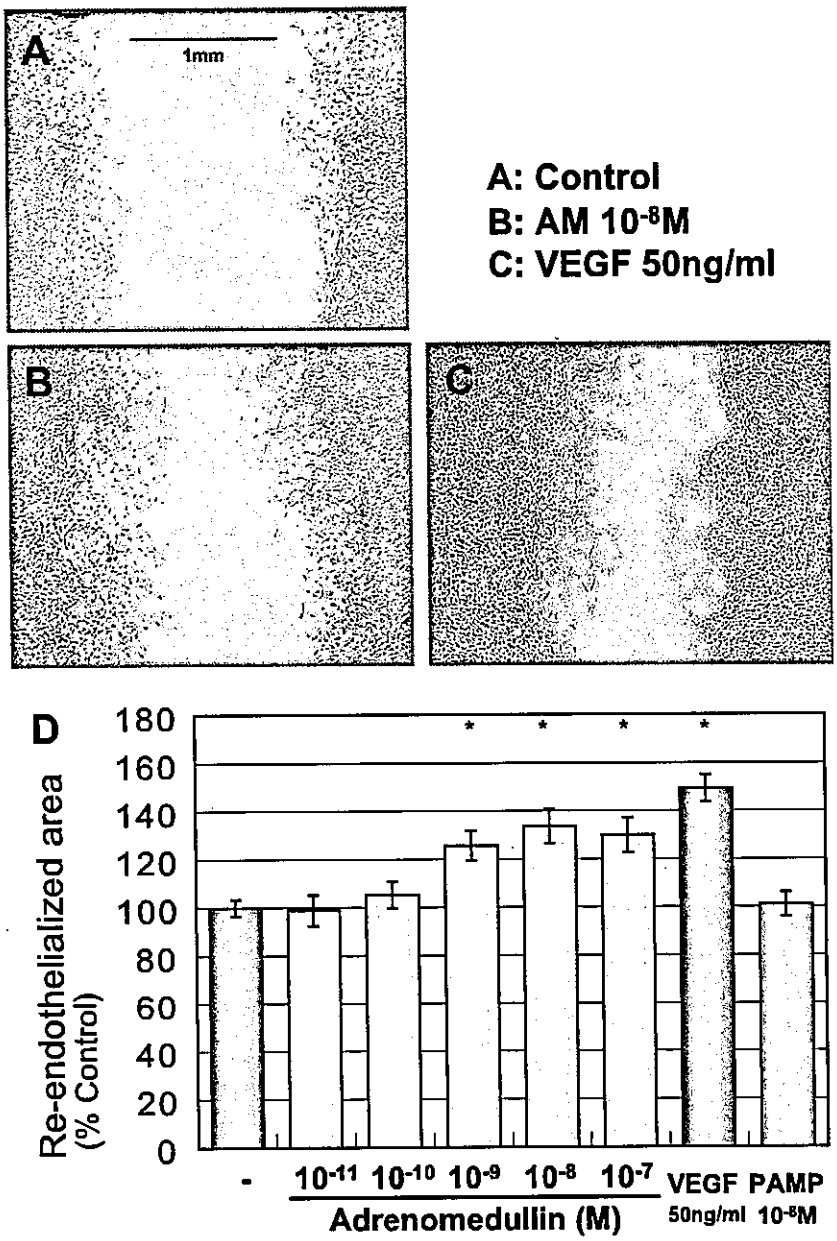

Fig. 2. Effect of AM on endothelial regeneration in wound healing assay in vitro. Wounded monolayer of HUVECs was incubated for 40 h. A–C: Representative photographs of re-endothelialized monolayer incubated for 40 h with the medium containing 0.5% FBS (control) (panel A), accompanied by AM (panel B), or VEGF (panel C). D: Dose-dependent effect of AM on endothelial regeneration in comparison to VEGF and PAMP. *: $P<0.01$ versus the control, $n=12$.

3.2. *AM promoted re-endothelialization of the wounded monolayer of HUVECs through a PKA- and PI3K-dependent pathway*

Fig. 2 shows the closure of wounded endothelium incubated with FBS 0.5% (control) (Fig. 2A), accompanied with AM (10^{-8} mol/l) (Fig. 2B), or VEGF (50 ng/ml) (Fig. 2C) for 40 h. Accelerated wound closure was observed in the group treated with AM, as well as that treated with VEGF. Fig. 2D shows the dose-dependent effect of AM on endothelial regeneration in comparison with VEGF and PAMP. AM promoted the wound closure significantly and dose-dependently. The increase of re-endothelialized area by 10^{-8} mol/l AM was 33.6%±7.1% over the control ($P<0.01$, $n=12$). On the other hand, PAMP, a hypotensive peptide that is synthesized from the same precursor of AM, had no significant effect on endothelial regeneration.

We next examined the effect of the same inhibitors at the same concentrations which were used in Akt phosphorylation assay and had a significant inhibitory effect on AM-induced Akt activation. The two AM antagonists and the inhibitors for PKA or PI3K at those concentrations suppressed AM (10^{-8} mol/l)-induced endothelial regeneration without affecting basal wound closure (Table 1).

In addition, 8-Br-cAMP (10^{-9} mol/l) mimicked the AM action to promote endothelial regeneration in wound healing assay (21.8%±5.0% over the control, $P<0.01$, $n=8$).

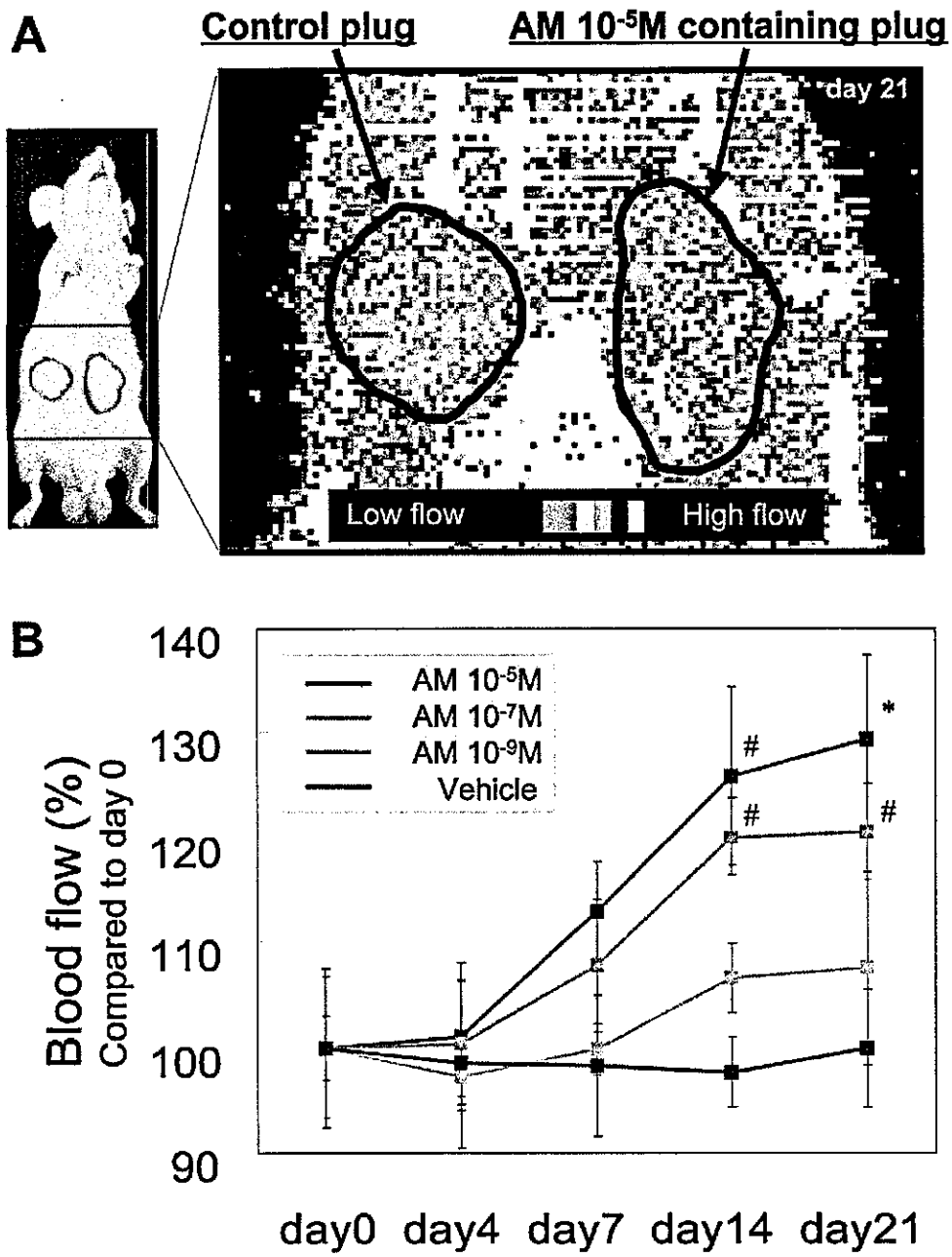

Fig. 3. Effect of AM on blood perfusion in murine gel plug assay. A: Blood flow measurement by a laser Doppler perfusion image analyzer. A representative view of a mouse injected with an AM-containing gel (10^{-5} mol/l) and a control gel is shown. The high-flow area is depicted in red to white and the low-flow in green to black. B: Time course of the effect of AM on blood flow in gel plugs. Blood flow on each day was measured by the laser Doppler perfusion image analyzer and compared to that on day 0. #: $P<0.05$; *: $P<0.01$ versus the blood flow on day 0. $n=12$ (AM 10^{-5} mol/l group), 8 (AM 10^{-7} mol/l and vehicle groups), and 4 (AM 10^{-9} mol/l group).

3.3. AM augmented blood flow in the plug through a PKA- and PI3K-dependent pathway

Fig. 3A demonstrates a representative image of the blood flow analysis of gel plugs on day 21. The AM-containing plug presented significantly higher blood perfusion compared to its control plug. The blood flow of the 10^{-5} mol/l AM-containing plug on day 21 was 29.4%±8.1% higher than that on day 0 ($P<0.01$, $n=12$; Fig. 3B).

The effects of the inhibitors on the AM-induced increase in blood flow were examined. Inclusion of the AM antagonists and the inhibitors for PKA or PI3K in AM-containing plugs significantly suppressed AM (10^{-7} mol/l)-induced augmentation of blood flow (Table 2).

The inhibitors at the doses used in the MATRIGEL plug assay had no significant effect on basal blood flow (Table 2) and the number of neo-vessels (data not shown) of gel plugs without AM. They did not have any significant toxic effects.

3.4. AM increased capillary density in gel plugs

Microscopic observation of whole and sliced plugs revealed

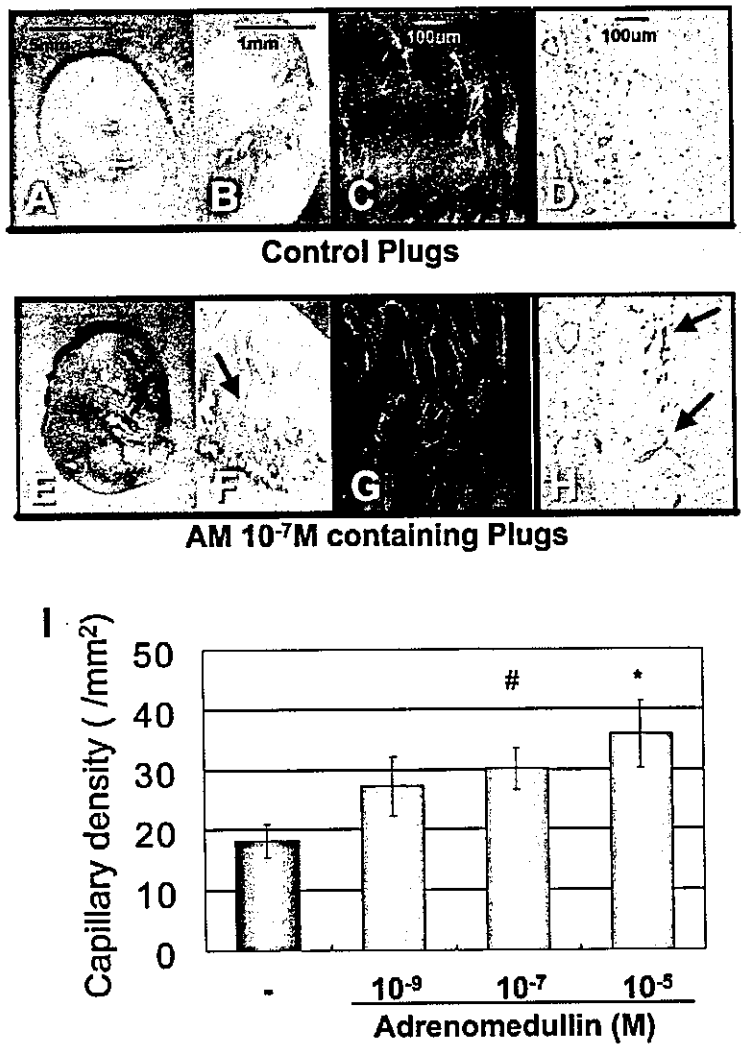

Fig. 4. Effect of AM on neo-vascularization in the gel plug. Gel plugs were harvested with underlying skin from mice on day 21 and angiogenic signs were microscopically examined. A–H: Representative images of a whole and sliced AM (10^{-7} mol/l)-containing plug (panels E and F) are shown, in comparison to the control plug (panels A and B). The plugs were stained with PECAM-1 to visualize neo-vessels. Immunochemically stained and fluorescent-labeled sections of an AM-containing plug (panels G and H) are shown, as compared to the control (panels C and D). The fluorescent-labeled sections were observed with a confocal microscope that can re-construct the 3D structure of small capillaries. I: Dose-dependent effect of AM on capillary density in the plugs determined by PECAM-1 immuno-reactivity on day 21. #: $P<0.05$; *: $P<0.01$ versus the control. $n=9$. Green: fluorescent-labeled PECAM-1 (panels C and G); brown: immunochemically stained PECAM-1 (panels D and H); arrows: neo-vessels in AM-containing plugs (panels F and H).

enhanced neo-vascularization in AM-containing plugs (Fig. 4E,F) compared to their control plugs (Fig. 4A,B). The capillary density estimated from PECAM-1 immuno-reactivity (Fig. 4D,H) was significantly and dose-dependently increased in AM-containing plugs (18.2 ± 2.8 per mm^2 in the control, 35.7 ± 5.7 per mm^2 in the 10^{-5} mol/l AM-containing plug on day 21; $P<0.01$ versus the control, $n=9$; Fig. 4I). We also confirmed increased capillary network in the AM-containing plug by observation with a confocal microscope that could visualize the 3D structure of capillaries of approximately 10 μm diameter (Fig. 4C,G).

4. Discussion

In this study, we showed that AM provokes endothelial Akt activation in a PKA- and PI3K-dependent manner and demonstrated that AM promotes endothelial regeneration in vitro and increases blood flow and capillary density in gel plugs in vivo through a PKA- and PI3K-dependent pathway.

AM-induced Akt activation in rat aortic tissues has been shown in a previous report [18]. In this study, we further confirmed that AM-induced Akt activation occurs in cultured endothelial cells. We also demonstrated that Akt is activated by the artificial wounds on HUVECs. Furthermore, we revealed that AM increases wound-induced Akt activation. Akt has been shown to regulate survival, migration, and nitric oxide production in endothelium [19]. In addition, constitutive Akt signaling in endothelium has been reported to be sufficient to promote angiogenesis in a rabbit hindlimb ischemia model [20]. Therefore, Akt activation in endothelium can be regarded as a key event in transduction of the angiogenic signal [21]. In the present study, AM-induced vascular regen-

Table 1
The effect of the AM antagonists and the inhibitors for PKA or PI3K on AM-induced endothelial regeneration

Treatment ($n=4$)	Re-endothelialized area (% control)	Treatment ($n=8$)	Re-endothelialized area (% control)
Control (FBS 0.5%)	100.0 ± 3.5	AM (10^{-8} mol/l)	132.6 ± 1.4[a]
+AM (22–52) (10^{-5} mol/l)	96.4 ± 5.4	+AM (22–52) (10^{-5} mol/l)	111.2 ± 7.4[b]
+CGRP (8–37) (10^{-5} mol/l)	103.3 ± 11.1	+CGRP (8–37) (10^{-5} mol/l)	119.8 ± 3.0[c]
+Rp-cAMP (10^{-5} mol/l)	104.0 ± 6.2	+Rp-cAMP (10^{-5} mol/l)	112.5 ± 11.7[b]
+PKA Inh. Peptide (5×10^{-7} mol/l)	101.7 ± 9.4	+PKA Inh. Peptide (5×10^{-7} mol/l)	113.0 ± 3.6[b]
+LY294002 (10^{-5} mol/l)	97.3 ± 14.7	+LY294002 (10^{-5} mol/l)	105.1 ± 6.6[b]
+Wortmannin (10^{-7} mol/l)	103.8 ± 13.1	+Wortmannin (10^{-7} mol/l)	103.0 ± 3.9[b]

Values are shown as mean ± S.E.M.
[a] $P<0.01$ versus the control.
[b] $P<0.01$ versus the AM (10^{-8} mol/l)-treated group without inhibitors.
[c] $P<0.05$ versus the AM (10^{-8} mol/l)-treated group without inhibitors.

Table 2
The effect of the AM antagonists and the inhibitors for PKA or PI3K on AM-induced augmentation of blood flow in gel plugs

Treatment ($n=4$)	Blood flow on day 21 (% control)	Treatment ($n=4$)	Blood flow on day 21 (% control)
Control	100.0 ± 0.0	AM (10^{-7} mol/l)	143.7 ± 5.5[a]
+AM (22–52) (10^{-4} mol/l)	101.1 ± 2.3	+AM (22–52) (10^{-4} mol/l)	104.1 ± 6.2[b]
+CGRP (8–37) (10^{-4} mol/l)	96.8 ± 10.1	+CGRP (8–37) (10^{-4} mol/l)	112.6 ± 3.7[b]
+Rp-cAMP (10^{-3} mol/l)	102.7 ± 11.7	+Rp-cAMP (10^{-3} mol/l)	113.2 ± 6.1[b]
+PKA Inh. Peptide (10^{-4} mol/l)	105.2 ± 6.1	+PKA Inh. Peptide (10^{-4} mol/l)	104.1 ± 9.8[b]
+LY294002 (10^{-3} mol/l)	100.1 ± 0.5	+LY294002 (10^{-3} mol/l)	109.3 ± 7.6[b]
+Wortmannin (10^{-5} mol/l)	101.2 ± 8.0	+Wortmannin (10^{-5} mol/l)	111.9 ± 7.4[b]

Values are shown as mean ± S.E.M.
[a] $P<0.01$ versus the control.
[b] $P<0.01$ versus AM (10^{-7} mol/l)-containing plugs without inhibitors.

eration both in vitro and in vivo was suppressed by PI3K inhibitors. Therefore, it is suggested that AM regulates neovascularization via enhancement of endothelial Akt activity following PI3K activation.

There are also several reports that imply the involvement of the cAMP/PKA cascade in vascular regeneration. However, whether PKA activation promotes or inhibits vascular regeneration is controversial [22,23]. In the present study, AM-induced vascular regeneration both in vitro and in vivo was significantly abrogated by the two PKA inhibitors, and 8-Br-cAMP simulated the effect of AM. Therefore, the cAMP/PKA cascade is supposed to have potency to promote vascular regeneration, at least in our experimental conditions. We also revealed that AM-induced Akt activation is suppressed by the inhibitors for not only PI3K but also for PKA. These results suggest the significance of the cAMP/PKA cascade on the regulation of Akt activity, which can induce vascular regeneration. The molecular mechanism in PKA-induced Akt activation is now under investigation.

In MATRIGEL plug assay, it has been reported that 10–100 times higher concentrations of substances than those used in cell culture experiments were required to exert enough influence in gel plugs [24,25]. Based on these previous reports, we planned to use higher concentrations of AM in MATRIGEL plug assay in vivo than in wound healing assay in vitro. As a result, the effective concentrations of AM were revealed to be 10^{-9}–10^{-7} mol/l in vitro and 10^{-7}–10^{-5} mol/l in vivo. The optimal concentrations of AM in vitro for cultured endothelial cells were similar to previous reports [26]. The difference between the effective concentrations in vitro and in vivo observed in our present study was also compatible with previous reports [24,25].

In conclusion, we demonstrated that AM provokes endothelial Akt activation and promotes vascular regeneration both in vitro and in vivo through a PKA- and PI3K-dependent pathway. These findings suggest the usefulness of AM as a new therapeutic agent for vascular injury, atherosclerotic diseases and tissue ischemia.

References

[1] Ross, R. (1993) Nature 362, 801–809.
[2] Carmeliet, P. (2000) Nat. Med. 6, 389–395.
[3] Suga, S., Nakao, K., Itoh, H., Komatsu, Y., Ogawa, Y., Hama, N. and Imura, H. (1992) J. Clin. Invest. 90, 1145–1149.
[4] Doi, K., Ikeda, T., Itoh, H., Ueyama, K., Hosoda, K., Ogawa, Y., Yamashita, J., Chun, T.H., Inoue, M., Masatsugu, K., Sawada, N., Fukunaga, Y., Saito, T., Sone, M., Yamahara, K., Kook, H., Komeda, M., Ueda, M. and Nakao, K. (2001) Arterioscler. Thromb. Vasc. Biol. 21, 930–936.
[5] Ohno, N., Itoh, H., Ikeda, T., Ueyama, K., Yamahara, K., Doi, K., Yamashita, J., Inoue, M., Masatsugu, K., Sawada, N., Fukunaga, Y., Sakaguchi, S., Sone, M., Yurugi, T., Kook, H., Komeda, M. and Nakao, K. (2002) Circulation 105, 1623–1626.
[6] Yamahara, K., Itoh, H., Chun, T.H., Ogawa, Y., Yamashita, J., Sawada, N., Fukunaga, Y., Sone, M., Yurugi-Kobayashi, T., Miyashita, K., Tsujimoto, H., Kook, H., Feil, R., Garbers, D.L., Hofmann, F. and Nakao, K. (2003) Proc. Natl. Acad. Sci. USA 100, 3404–3409.
[7] Kook, H., Itoh, H., Choi, B.S., Sawada, N., Doi, K., Hwang, T.J., Kim, K.K., Arai, H., Baik, Y.H. and Nakao, K. (2003) Am. J. Physiol. Heart Circ. Physiol. 284, 1388–1397.
[8] Kitamura, K., Kangawa, K., Kawamoto, M., Ichiki, Y., Nakamura, S., Matsuo, H. and Eto, T. (1993) Biochem. Biophys. Res. Commun. 192, 553–560.
[9] Eto, T. (2001) Peptides 22, 1693–1711.
[10] Shindo, T., Kurihara, H., Maemura, K., Kurihara, Y., Kuwaki, T., Izumida, T., Minamino, N., Ju, K.H., Morita, H., Oh-hashi, Y., Kumada, M., Kangawa, K., Nagai, R. and Yazaki, Y. (2000) Circulation 101, 2309–2316.
[11] Shindo, T., Kurihara, Y., Nishimatsu, H., Moriyama, N., Kakoki, M., Wang, Y., Imai, Y., Ebihara, A., Kuwaki, T., Ju, K.H., Minamino, N., Kangawa, K., Ishikawa, T., Fukuda, M., Akimoto, Y., Kawakami, H., Imai, T., Morita, H., Yazaki, Y., Nagai,

R., Hirata, Y. and Kurihara, H. (2001) Circulation 104, 1964–1971.
[12] Shimosawa, T., Shibagaki, Y., Ishibashi, K., Kitamura, K., Kangawa, K., Kato, S., Ando, K. and Fujita, T. (2002) Circulation 105, 106–111.
[13] Nakayama, M., Takahashi, K., Murakami, O., Murakami, H., Sasano, H., Shirato, K. and Shibahara, S. (1999) Clin. Sci. (Lond.) 97, 247–251.
[14] Cormier-Regard, S., Nguyen, S.V. and Claycomb, W.C. (1998) J. Biol. Chem. 273, 17787–17792.
[15] Miyashita, K., Itoh, H., Sawada, N., Fukunaga, Y., Sone, M., Yamahara, K., Yurugi, T. and Nakao, K. (2003) Hypertens. Res. 26, S93–8.
[16] Sawada, N., Itoh, H., Yamashita, J., Doi, K., Inoue, M., Masatsugu, K., Fukunaga, Y., Sakaguchi, S., Sone, M., Yamahara, K., Yurugi, T. and Nakao, K. (2001) Biochem. Biophys. Res. Commun. 280, 798–805.
[17] Passaniti, A., Taylor, R.M., Pili, R., Guo, Y., Long, P.V., Haney, J.A., Pauly, R.R., Grant, D.S. and Martin, G.R. (1992) Lab. Invest. 67, 519–528.
[18] Nishimatsu, H., Suzuki, E., Nagata, D., Moriyama, N., Satonaka, H., Walsh, K., Sata, M., Kangawa, K., Matsuo, H., Goto,A., Kitamura, T. and Hirata, Y. (2001) Circ. Res. 89, 63–70.
[19] Morales-Ruiz, M., Fulton, D., Sowa, G., Languino, L.R., Fujio, Y., Walsh, K. and Sessa, W.C. (2000) Circ. Res. 86, 892–896.
[20] Kureishi, Y., Luo, Z., Shiojima, I., Bialik, A., Fulton, D., Lefer, D.J., Sessa, W.C. and Walsh, K. (2000) Nat. Med. 6, 1004–1010.
[21] Dimmeler, S. and Zeiher, A.M. (2000) Circ. Res. 86, 4–5.
[22] Amano, H., Ando, K., Minamida, S., Hayashi, I., Ogino, M., Yamashina, S., Yoshimura, H. and Majima, M. (2001) Jpn. J. Pharmacol. 87, 181–188.
[23] Kim, S., Bakre, M., Yin, H. and Varner, J.A. (2002) J. Clin. Invest. 110, 933–941.
[24] Wajih, N. and Sane, D.C. (2003) Blood 101, 1857–1863.
[25] Lee, M.J., Thangada, S., Claffey, K.P., Ancellin, N., Liu, C.H., Kluk, M., Volpi, M., Sha'afi, R.I. and Hla, T. (1999) Cell 99, 301–312.
[26] Michibata, H., Mukoyama, M., Tanaka, I., Suga, S., Nakagawa, M., Ishibashi, R., Goto, M., Akaji, K., Fujiwara, Y., Kiso, Y. and Nakao, K. (1998) Kidney Int. 53, 979–985.

International Journal of Urology (2003) **10**, 544–546

Case Report

Successful treatment of primary aldosteronism due to computed tomography-negative microadenoma

KOJI NISHIZAWA,[1] EIJIRO NAKAMURA,[1] TAKASHI KOBAYASHI,[1] TOSHIYUKI KAMOTO,[1] AKITO TERAI,[1] TOSHIRO TERACHI,[1] OSAMU OGAWA,[1] HIROSHI ITOH[2] AND KAZUWA NAKAO[2]

Departments of [1]Urology and [2]Medicine and Clinical Science, Graduate School of Medicine, Kyoto University, Kyoto, Japan

Abstract We report a case of aldosterone-producing microadenoma that was correctly diagnosed and thus treated less invasively by laparoscopic adrenalectomy. A 58-year-old woman presented with palpitation and muscular weakness. She exhibited hypertension, hypokalemia and increased aldosterone excretion with suppressed renin activity. Therefore, primary aldosteronism was suggested. Although adrenal scintigram and computed tomography findings in the adrenal glands were normal, adrenal venous sampling tests indicated an overproduction of aldosterone in the right adrenal gland. We diagnosed an aldosterone-producing microadenoma in the right adrenal gland and performed an adrenalectomy. The patient became normotensive postoperatively and histopathological examination demonstrated a microadenoma, 5 mm in diameter.

Key words laparoscopic adrenalectomy, microadenoma, primary aldosteronism.

Introduction

Primary aldosteronism (PA) encompasses disorders characterized by hypertension, hypokalemia and increased aldosterone excretion with suppressed renin activity.[1,2] It is important to distinguish aldosterone-producing adenoma (APA) from idiopathic hyperaldosteronism (IHA) because patients with APA can be successfully managed by surgical treatment alone. However, some cases of APAs, particularly those caused by a microadenoma, are overlooked because this kind of adenoma is difficult to detect by imaging studies such as computed tomography (CT). We report a case of APA caused by a microadenoma that was correctly diagnosed and thus, treated less invasively by laparoscopic adrenalectomy.

Correspondence: Osamu Ogawa MD, Professor and Chairman, Department of Urology, Graduate School of Medicine, Kyoto University, Shogoin Kawahara-cho 54, Sakyo-ku, Kyoto City 606-8507, Japan.
Email: ogawao@kuhp.kyoto-u.ac.jp
Received 9 May 2002; accepted 24 March 2003.

Case report

A 58-year-old woman consulted our hospital with complaints of palpitation and muscular weakness. At her initial presentation, hypertension and hypokalemia were apparent. Plasma aldosterone concentration was examined and found to be 225 pg/mL (normal range, 30–160 pg/mL). No abnormal findings, such as 17-OHCS or 17-KS in urine, were observed in any of the other laboratory examinations. Thus, the patient was examined by an adrenal scintigram using ^{131}iodine adosterol and 3-mm-thick CT sections to detect aldosterone-producing adenomas (Fig. 1). However, these examinations did not detect any abnormal findings in the adrenal glands. To further examine the causes of PA, adrenal venous sampling tests with adrenocorticotropic hormone (ACTH) stimulation were performed.[3] The aldosterone concentration from the catheterized left adrenal vein was 291 and the calculation of an aldosterone/cortisol (A/C) ratio was 4.9 (below 5, in the normal range). After stimulation, the aldosterone concentration from the right and left adrenal veins increased from 1195 to 5 4198 and 291 to 1475 ng/dL, and the A/C ratios from 10 to 149 and 4.9 to 13.2, respectively. The

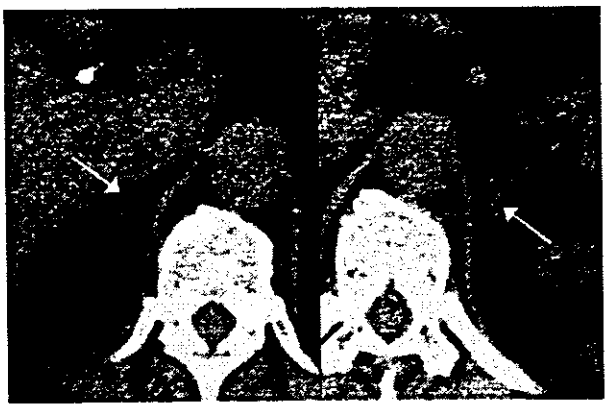

Fig. 1 Enhanced computed tomography of a 58-year-old woman with aldosterone-producing microadenoma shows no mass in either adrenal gland (arrows).

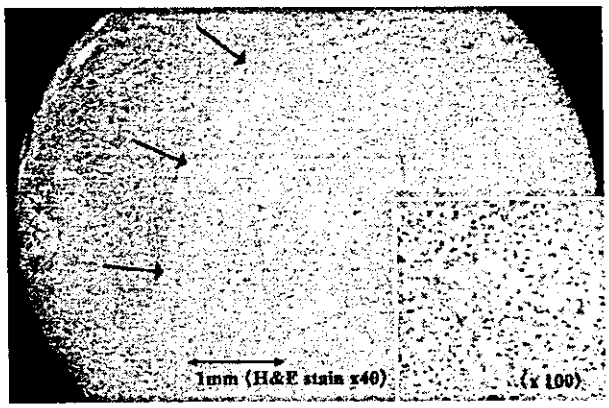

Fig. 2 Histopathological findings: solitary adenoma consisting mainly of clear cells and a small number of compact cells (H&E × 40).

overproduction of aldosterone in the right adrenal gland was highly suggestive of an aldosterone-producing microadenoma in the right adrenal gland.

After spironolactone intake alone, the patient's blood pressure decreased from 160/100 to 135/86 mmhg, and her symptoms were relieved. This was predictive of a favorable outcome by surgical management.[4] Therefore, transperitoneal laparoscopic right adrenalectomy was performed following operative procedures described previously.[5] The operation lasted for 183 min and there was little blood loss. The patient started to walk and eat on the first postoperative day. Histopathological examination indeed exhibited a microadenoma 5 mm in diameter, consisting mainly of clear cells and partly of compact cells with microscopic findings compatible with APA. The adenoma was composed of cells resembling zona glomerulosa or the hybrid type of cell. The zona fasciculata of the attached cortex showed hyperplasia and was diffusely widened (Fig. 2). After adrenalectomy, serum aldosterone level decreased from 225 to 48 pg/mL and blood pressure settled at 132/72 mmhg without spironolactone. Serum potassium concentration increased from 3.1 to 3.6 mEp/mL. Thus, plasma aldosterone levels, serum potassium and blood pressure normalized postoperatively.

Discussion

From a therapeutic point of view, an accurate diagnosis of the causes of PA is important because surgical management is a successful treatment for most patients with APA.[4] An adenoma that cannot be proved by thin-section CT, but can be proved by clinical and pathological findings is defined as a microadenoma. These adenomas are usually smaller than 1 cm in diameter, and their lateralization can be proved by venous sampling with or without stimulation.[1-3] Generally an adenoma exists in the adrenal cortex with a tenuous capsule, and its cut surface is characteristically bright yellow.[4] Recent advances in CT scanning make it possible to detect up to 90% of adenomas that cause APA.[6] Magnetic resonance imaging (MRI) may be more accurate at localizing small adenomas than CT.[7,8] Thus, it is possible that the adenoma described herein, which was up to 5 mm in diameter, might have been described on MRI.

Because adenomas smaller than 1 cm in diameter are easily missed, adrenal venous sampling tests are inevitable in some patients.[1,2,4] Indeed, many patients exhibited excessive secretion of aldosterone in this sampling, irrespective of prior normal adrenal gland findings on CT imagings.[9] A unilateral excess of aldosterone does not always indicate the presence of an aldosterone producing adenoma because the possibility of adrenal hyperplasia remains. However, unilateral adrenalectomy is usually performed because it will also improve hypertension, even in the latter case.[2,3] After adrenalectomy, a diagnosis of APA can be confirmed by histopathological analysis, changes in serum aldosterone levels and potassium, and blood pressure. In histopathological analysis, it is known that immunohistochemical study, especially for 3-beta-hydroxysteroid dehydrogenase, is helpful for making a deferential diagnosis between an aldosterone-producing adenoma and idiopathic hyperaldosteronism.[10]

Evidence is accumulating that aldosteron-producing microadenomas are present in most patients diagnosed with PA and that the prevalence of this disease among hypertensive disorders[4] could be higher than

expected.[2,9] Nishikawa and Omura diagnosed 55 cases of PA (5.4%) by adrenal venous sampling tests from 1020 patients initially diagnosed with essential hypertension.[9] Among these 55 patients, aldosteron-producing microadenomas caused PA in as many as 26 cases (47%). These results allow for the possibility that surgical management alone could cure a significant proportion of hypertensive patients if correctly diagnosed. Thus, the accurate diagnosis of aldosteron-producing microadenomas followed by laparoscopic adrenalectomy has considerable potential in the treatment of hypertensive diseases.

References

1 Sheaves R, Goldin J, Reznek RH *et al.* Relative value of computed tomography scanning and venous sampling in establishing the cause of primary hyperaldosteronism. *Eur. J. Endocrinol.* 1996; **134**: 308–13.

2 Young WF, Stanson AW, Grant CS, Thompson GB, van Heerden JA. Primary aldosteronism: adrenal venous sampling. *Surgery* 1996; **120**: 913–20.

3 Doppman JL, Gill JR, Miller DL *et al.* Distinction between hyperaldosteronism due to bilateral hyperplasia and unilateral aldosteronoma: reliability of CT. *Radiology* 1992; **184**: 677–82.

4 Ganguly A. Primary aldosteronism. *N. Engl. J. Med.* 1998; **339**: 1828–34.

5 Terachi T, Matsuda T, Terai A *et al.* Transperitoneal laparoscopic adrenalectomy: experience in 100 patients. *J. Endourol.* 1997; **11**: 361–5.

6 Radin DR, Manoogian C, Nadler JL. Diagnosis of primary hyperaldosteronism: importance of correlating CT findings with endocrinologic studies. *AJR Am. J. Roentgenol.* 1992; **158**: 553–7.

7 Nishikawa T, Omura M. Clinical characteristics of primary aldosteronism: its prevalence and comparative studies on various causes of primary aldosteronism in Yokohama Rosai Hospital. *Biomed. Pharmacother.* 2000; **54**: 83–5.

8 Rossi GP, Chiesura-Corona M, Tregnaghi A *et al.* Imaging of aldosterone-secreting adenomas: a prospective comparison of computed tomography and magnetic resonance imaging in 27 patients with suspected primary aldosteronism. *J. Hum. Hypertens.* 1993; **7**: 357–63.

9 Nakao Y, Abe I, Kobayashi K *et al.* Evaluation of the localizing procedures of primary aldosteronism. *Nippon Jinzo Gakkai Shi.* 1993; **35**: 281–6.

10 Omura M, Kagami S, Seki N *et al.* Case of primary aldosteronism caused by adrenal microadenoma that permitted clinical observation from onset. *Nippon Naika Gakkai Zasshi* 1999; **88**: 2474–5.

Available online at www.sciencedirect.com

SCIENCE DIRECT

European Journal of Pharmacology 508 (2005) 255–265

www.elsevier.com/locate/ejphar

Therapeutic potential of thiazolidinediones in activation of peroxisome proliferator-activated receptor γ for monocyte recruitment and endothelial regeneration

Tokuji Tanaka[1], Yasutomo Fukunaga[1], Hiroshi Itoh*, Kentaro Doi, Jun Yamashita, Tae-Hwa Chun, Mayumi Inoue, Ken Masatsugu, Takatoshi Saito, Naoki Sawada, Satsuki Sakaguchi, Hiroshi Arai, Kazuwa Nakao

Department of Medicine and Clinical Science, Kyoto University Graduate School of Medicine, 54 Shogoin Kawahara-cho, Sakyo-ku, Kyoto 606-8507, Japan

Received 8 July 2004; received in revised form 18 October 2004; accepted 28 October 2004
Available online 30 December 2004

Abstract

Thiazolidinediones, a new class of antidiabetic drugs that increase insulin sensitivity, have been shown to be ligands for peroxisome proliferator-activated receptor γ (PPARγ). Recent studies demonstrating that PPARγ occurs in macrophages have focused attention on its role in macrophage functions. In this study, we investigated the effect of thiazolidinediones on monocyte proliferation and migration in vitro and the mechanisms involved. In addition, we examined the therapeutic potentials of thiazolidinediones for injured atherosclerotic lesions. Troglitazone and pioglitazone, the two thiazolidinediones, as well as 15-deoxy-Δ12,14-prostaglandin J2 inhibited in a dose-dependent manner the serum-induced proliferation of THP-1 (human monocytic leukemia cells) and of U937 (human monoblastic leukemia cells), which permanently express PPARγ. These ligands for PPARγ also significantly inhibited migration of THP-1 induced by monocyte chemoattractant protein-1 (MCP-1). Troglitazone and 15-deoxy-Δ12,14-prostaglandin J2 significantly suppressed the mRNA expression of the MCP family-specific receptor CCR2 (chemokine CCR2 receptor) in THP-1 at the transcriptional level. Furthermore, troglitazone significantly inhibited MCP-1 binding to THP-1. Oral administration of troglitazone to Watanabe heritable hyperlipidemic (WHHL) rabbits after balloon injury suppressed acute recruitment of monocytes/macrophages and accelerated re-endothelialization. These results suggest that thiazolidinediones have therapeutic potential for the treatment of diabetic vascular complications.

Keywords: Thiazolidinedione; PPARγ; MCP-1; CCR2; Macrophage; Insulin resistance

1. Introduction

Recruitment of circulating monocytes and their proliferation and differentiation into macrophages are not only the central events for initiation and progression of atherosclerosis, but have also been recently recognized as crucial pathogenic events in both diabetic micro- and macroangiopathy. Monocyte chemoattractant protein (MCP)-1 is a member of the C-C branch (or β) of the chemokine family and a potent monocyte and lymphocyte chemoattractant, which is expressed abundantly in atherosclerosic lesions (Nelken et al., 1991). MCP-1 initiates signal transduction through binding to the chemokine CCR2 receptor (CCR2) (Charo et al., 1994). In a study of CCR2 knockout mice, markedly fewer macrophages were present in the aorta of CCR2−/−, apoE−/− double knockout mice than in that of apoE−/− mice (Boring et al., 1998). Moreover, an independent study demonstrated that MCP-1−/− mice, when crossed with LDL receptor−/− mice, had smaller lesions and a significant reduction of macrophages in the lesions (Gu et al., 1998). These findings indicate the direct role of MCP-1 and CCR2 in monocyte recruitment and atherosclerosis.

* Corresponding author. Tel.: +81 75 751 3170; fax: +81 75 771 9452.
E-mail address: hiito@kuhp.kyoto-u.ac.jp (H. Itoh).
[1] These two authors contributed equally to this work.

0014-2999/$ - see front matter © 2004 Elsevier B.V. All rights reserved.
doi:10.1016/j.ejphar.2004.10.056

Thiazolidinediones are a new class of antidiabetic agents that increase sensitivity to insulin (Nolan et al., 1994). Insulin resistance has been attracting attention as the common casual factor not only for diabetes mellitus but also for hypertension, hyperlipidemia and obesity, all of which are risk factors for atherosclerosis (DeFronzo and Ferrannini, 1991). Recently, thiazolidinediones have been shown to be the ligands for peroxisome proliferator-activated receptor γ (PPARγ), which is a member of the nuclear receptor superfamily of ligand-activated transcription factors and has been identified as the functional receptor in antidiabetic action of thiazolidinediones (Lehmann et al., 1995).

PPARγ and the retinoid X receptor contain a heterodimer to bind regulatory elements in the promoter region of a number of adipocyte-specific genes and stimulate transcription (Tontonoz et al., 1994). In a previous study, we cloned rat PPARγ and detected down-regulation of PPARγ mRNA by several cytokines (Tanaka et al., 1999). Recent studies have demonstrated that PPARγ is expressed in cells of monocyte/macrophage lineage (Ricote et al., 1998; Tontonoz et al., 1998), and that oxidized low density lipoprotein (oxLDL), which plays a central role in atherogenesis, can regulate PPARγ-dependent gene transcription (Nagy et al., 1998). We recently reported that oxLDL potentiates, through the activation of PPARγ, the expression of vascular endothelial growth factor (VEGF) in human endothelial cells and in monocytes/macrophages (Inoue et al., 2001). Another study demonstrated that the administration of troglitazone, one of the thiazolidinediones, to Watanabe heritable hyperlipidemia (WHHL) rabbits and high fat-fed low density lipoprotein receptor or apo E knockout mice inhibits progression of atherosclerosis (Shiomi et al., 1999; Chen et al., 2001; Collins et al., 2001). All of these studies indicate the significance of PPARγ in monocyte and macrophage functions and atherogenesis.

The objective of the study presented here was to determine the effect of thiazolidinediones on the migration and proliferation of monocytes/macrophages and to investigate the molecular mechanism of the effect of thiazolidinediones on MCP-1-induced monocyte migration, with the focus on the expression of CCR2. Furthermore, we used WHHL atherosclerotic rabbits for an in vivo investigation of the therapeutic potentials of thiazolidinediones for acute monocyte recruitment and infiltration as well as for endothelial regeneration after acute vascular injury.

2. Materials and methods

2.1. Cell culture

THP-1 (human monocytic leukemia cells) and U937 (human monoblastic leukemia cells) were obtained from ATCC and cultured as previously reported (Inoue et al., 2001), with or without the following agents: troglitazone (Sankyo, Tokyo, Japan), pioglitazone (Takeda Chemical Industries, Osaka, Japan), 15-deoxy-Δ12,14-prostaglandin J2 (Sigma, St. Louis, MO), which is one of the natural ligands of PPARγ, or 9-*cis*-retinoic acid (Sigma), which is the ligand of the retinoid X receptor.

2.2. Northern blot analysis

Total cellular RNA was isolated from cultured cells using TRIzol reagents (Gibco BRL, Gaithersburg, MD). Northern blot analysis was performed as described elsewhere (Tanaka et al., 1999). The human PPARγ probe consisted of an 858-base pair fragment of the cDNA corresponding to nucleotides 329–1186 of the human PPARγ1 cDNA. The human CCR2 probe consisted of a 939-base pair fragment of the CCR2 cDNA corresponding to nucleotides 1–939. A human β-actin probe (Wako, Japan) was used to monitor the amount of total RNA in each sample.

2.3. Establishment of U937 cells permanently expressing PPARγ

U937 cells permanently expressing PPARγ were established by using the PPARγ expression vector (pCMX-mPPARγ), which contains a cytomegalovirus enhancer and mouse full-length PPARγ cDNA, as we previously reported and explained in detail (Inoue et al., 2001).

2.4. Chemotaxis assay

The cell migration was evaluated with the modified Boyden chamber technique using a 96-well chemotaxis chamber (Neuroprobe, Cabin John, MD) with 50 μl of cell suspension (2×10^7 cells/ml cells in Roswell Park Memorial Institute medium (RPMI)), as previously reported by us (Sawada et al., 2000).

2.5. Equilibrium binding analysis

The cells were suspended at a density of 2×10^7 cells/ml in 200 μl of binding buffer containing 0.1% bovine serum albumin. The cells were incubated with 0.02 nM ^{125}I-MCP-1 and various amounts of unlabelled ligand for 90 min at 25 °C. All assays were done in triplicate, and binding data were examined with the Ligand Assistance Program (Ligand Pharmaceuticals, Charlotte, NC) or Scatchard analysis.

2.6. Balloon angioplasty and troglitazone administration

Homozygous male WHHL rabbits (10 months old, 3.6±0.1 kg) were used for this study. The rabbits were supplied by Sankyo Pharmaceutical. All animals used in the present study were treated with humane care in compliance with the *Guide for the Care and Use of Laboratory Animals* prepared by the National Academy of Sciences and published by the National Institutes of Health (NIH